1497

Fabrication of microelectrode arrays for electrophysiological monitoring of hippocampal organotypic slice cultures by interface

A dissertation
submitted to the Faculty of Sciences of the University of Neuchâtel,
in fulfillment of the requirements for the degree of "Docteur ès Sciences"

by

Pierre Thiébaud
Diplomé en électronique-physique de l'Université de Neuchâtel

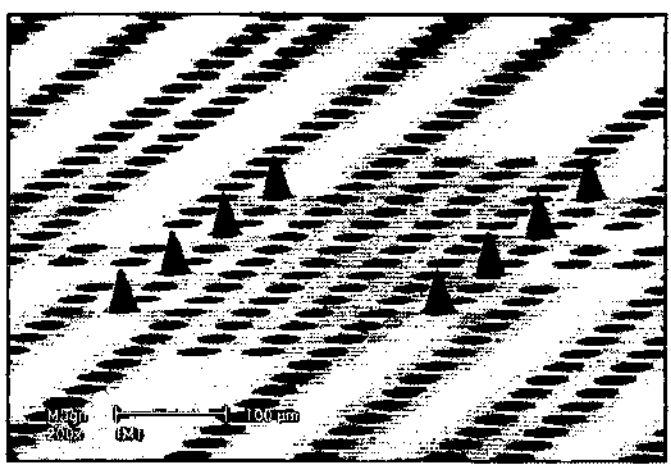

Institute of Microtechnology
University of Neuchâtel
Rue Jaquet-Droz 1, CH-2007 Neuchâtel
Switzerland

1999

IMPRIMATUR POUR LA THÈSE

Fabrication of microelectrode arrays for electrophysiological monitoring of hippocampal organotypic slice cultures by interface

de M. Pierre Thiébaud

UNIVERSITÉ DE NEUCHÂTEL

FACULTÉ DES SCIENCES

La Faculté des sciences de l'Université de Neuchâtel sur le rapport des membres du jury,

Mme. M. Koudelka-Hep (directrice de thèse),
MM. N. de Rooij et M. Grattarola (Uni. Gênes I)

autorise l'impression de la présente thèse.

Neuchâtel, le 15 novembre 1999

Le doyen:

J.-P. Derendinger

Abstract

Considerable progress has been accomplished in the past few decades in the development of microelectrode arrays for neurophysiological applications. Using photolithographic patterning of gold, platinum and indium tin oxide thin-films, microelectrodes having precisely controlled dimensions have been realised on various substrates (glass, plastics, silicon). Their utility for extracellular activity recording of *in vitro* cultured nerve cells was fully demonstrated and some of them are now commercially available.

With a view to enlarging the application scope of these devices, this work describes a new development in which the microelectrodes arrays are embedded on a micromachined porous silicon substrate. The role of the porosity is to improve the gas exchange and accessibility of the nutritive solution to the cell/solution interface. All this is required to perform organotypic cultures by interface. Using deep reactive ion etching, perforated holes of 35-40 μm in diameter have been realised through the whole thickness of a silicon wafer resulting in a mechanically stable substrate with porosities up to 35 %.

Another aspect considered in this work is the fabrication of arrays of protruding micro-electrodes enabling, to a certain extent, tissue slice penetration. The expected benefit of these 3-dimensional electrodes is a better interfacial contact between electrode and cells. In this context, two widely different technological approaches have been investigated. First, an electrochemical deposition of bright platinum "hillocks" (20 μm height) and secondly, platinum-tip microelectrodes realised using the silicon anisotropic etching technology (47 μm height).

In order to evaluate these devices, the viability of organotypic cultures has been tested using hippocampus slices of rats and the extracellular recordings carried out by means of the microelectrodes arrays.

Table of contents

Abstract

Table of contents

1. Introduction

The understanding of the functioning mechanisms of the nervous system represents one of the most challenging subject and aroused the interest of a great number of researchers. A lot of devices and methods were developed and they resulted in important progresses in this field. For several decades, the microtechnology has proposed a new approach for the fabrication of these devices, especially for the detection of the neurons' extracellular electrical activity. This chapter will describe the context of this present work by presenting already developed micromachined devices as well as by describing the classical methods of measurement and their respective advantages and drawbacks. A book treating the microtechnology in this field [1] and some web sites can be consulted for recent information [2, 3].

1.1. Microtechnology for neuronal applicationa

With the small size of structures, comparable to the size of the neurons, which can be realised by microtechnology and the progress in this field, many different devices were developed for a great variety of applications linked to neuronal tissues. Some of them will be presented in this paragraph.

Materials

Many of the layers commonly used in microfabrication technology are biocompatible. This means that they show no neurotoxicity which could lead to the death of the cells. Some of the most currently used materials are reported here (non exhaustive list among a lot of tested materials [4, 5]):

- Substrate materials: silicon, glass, plastics
- Passivation layers: silicon nitride, silicon dioxide
- Conductor materials: platinum, gold, iridium, indium-tin oxide

The standard integrated circuit materials such as silicon, silicon nitride, silicon dioxide, are involved in a lot of applications because their fabrication processes are well known. Moreover attempts with some polymers as substrate or passivation were performed. For instance polyimide was used, but some problems appeared on long term with moisture and ionic contaminants, allowing only short term measurements to be performed [6, 7, 8]. A new epoxy based photoresist called EPON SU-8 shows a better ionic stability and an acceptable biocompatibility [9, 10]. Silicon nitride is a better insulator compared with silicon dioxide and polyimide in order to avoid ionic migration when the device is put in saline solution. However under small applied electric fields, silicon nitride anodises in the solution to form a silicon dioxide layer which become hydrated with time. This reaction can be avoided with a layer of silicon dioxide under the silicon nitride [11].

The electrodes, used to record the electrical activity of the neurons or to perform their stimulation, should avoid all chemical reactions with the tissue. For that reason many noble metals are used. These electrodes should show good electrical characteristics, in particular a low impedance. This impedance is mainly linked to the surface of the metal-liquid interface like it will be described in the chapter 4.2. In some experiments, the tissue has to be observed by using microscope with a bottom side illumination (diascopic illumination). For that purpose, transparent materials were selected for these particular devices. Usually the substrate consists of glass and the conductive material is indium thin oxide (ITO). The main drawback of this conductive transparent material is a higher electrical resistivity.

In vivo devices

Mainly two types of *in vivo* devices were developed. The first category consisted in tools for regeneration of axons and fibres. This regeneration occurs when the two ends of a cut nerve are placed in close proximity. If a membrane with holes is placed in between, axons regenerate through them.

With electrodes placed adjacent to the holes, recording and stimulation of individual axons can be achieved [12, 13, 14]. Another category was the microelectrodes insertable into the tissues. They consisted in several electrodes embedded on a probe which has a typical size in the order of millimetres in length, several tens of micrometers large, and some micrometers thick. A single probe can be designed [15, 16, 8] or an array of them to form 2-dimensional device [17, 11]. Different methods can be used to make three dimensional structures. One consisted of a microassembly of planar silicon multishank microprobes which are precisely positioned through a micromachined platform [18]. Another one was made by simply sawing the substrate to form vertical column then shaped by chemical etching [19]. The main application of these devices are the implantation in the cerebral cortex [20]. The effects of the implantation in the tissue were also investigated [21].

In vitro devices - microelectrode array (MEA)

The *in vitro* devices consist in biocompatible substrate with a microelectrodes array (MEA) embedded on it. Neural cells can be deposited on this substrate and kept alive. The application field of these MEA is the monitoring of extracellular neuronal activity in vitro. This follows both orientations: research and application. The former consists of a purely scientific interest in monitoring of spontaneous and evoked electrophysiological activity, over extended periods of time and under different culturing conditions. The latter intends to test the biological effect of toxicological and pharmaceutical agents on neurons.

The first reported micromachined device adapted for the culture of cells and the monitoring of the electrical activity was fabricated around 1970 [22]. It consisted of platinised gold MEA, embedded on a glass substrate and passivated by a photoresist. The activity of a dissociated culture of chick heart cells was detected. Following this first achievement, measurements on neurons, also in dissociated culture, were performed [23, 24]. Similar realisations were successfully tested [25] based on the use of indium-tin oxide as conductive

material with a plated gold at the recording sites [26]. The stimulation of the cells using the microelectrodes was achieved [27], also on fresh hippocampal slices [28]. Several devices were developed to control the network formed by the cells in dissociated cultures. To control the growth of the neurites, mechanical guiding structures were formed using photolithography techniques [29, 30, 31]. The same guiding effect can be obtained by changing the adhesion proprieties of the substrate. In this way, a preferred growth area can be designed [32, 33]. Wells were microfabricated on electrodes to implant the neurons in them. Thus the somas of the neurons are kept in a known position, while the fibres spread to obtain interconnections [34]. Devices to move cells by means of electrical fields were also developed [35]. Improvement was performed in the design of culturing chambers. They include perfusion of medium and control of the atmosphere to allow longer term survival [36]. An original approach consists of the integration of a standard culturing substrate with a printed circuit including electrodes. These electrodes are bigger than those made by microfabrication but their price is lower [37]. The development of the MEA is also enhanced by the progresses of data processing which allow the acquisition of signals measured on a greater number of electrodes [38]. Commercially available devices were developed and sold in Germany [39, 40] by Multi Channel Systems and in Japan [41] by Panasonic. The first one consists of an array of 60 gold microelectrodes, each 10 μm wide and spaced by 100 μm, covered with platinum black. This MEA is embedded on a quartz substrate and the passivation of the gold is in silicon nitride. The second system includes 64 platinized ITO microelectrodes of 50 μm wide and spaced by 150 μm. In this case, the substrate is in glass and the passivation layer in polyimide. The common characteristic of all these MEA is the non porous nature of the substrate. Thus, for biological reasons explained in paragraph 2.1., only dissociated cells or fresh slices were being cultured on these devices. For the most recent ones, organotypic immersed cultures, these be performed in a

rotating incubator and long term survival can be achieved [42, 43]. To perform an organotypic culture by interface, the substrate has to be porous to allow a liquid flux through it. The only realisation of such a device, consists of a perforated flexible membrane in polyimide. It was reported that with a porosity of 6% with holes' sizes ranging from 30 μm by 30 μm up to 30 μm by 200 μm, the time of survival of a rat's hippocampus was in an average of 12 h compared with non-porous devices with an average of 2 h [44]. This shows that an access of the culture medium on the one hand and a gas exchanges through the substrate on the other hand, enhance the conditions of survival of the neurons.

Electrodes

The size of the electrodes is a compromise regarding both biological and electrical considerations. The electrode should be as small as possible and as close as possible to the cells to obtain information from a localised point. But this electrode should have a sufficient surface in order to detect electrical signals with an acceptable signal to noise ratio. A good isolation between the electrodes and the culture medium must also be obtained. To improve the quality of the neural signal, the electrode impedance should be reduced by, for instance, changing the surface morphology. For that reason, the electrodes have been platinised since their first realisations, by a layer of an electrodeposited black platinum [22]. The platinisation lowers the interface impedance by enlarging the surface of contact, and increases therefore the level of the recorded signal without changing the geometrical area of the electrode. For instance the impedance of a gold electrode of 10 μm in diameter is decreased from 4 MΩ to 400 kΩ at 1 kHz after platinisation [39]. For similar reason gold plating was also performed [26]. Any process which induces roughness on the surface reduces the impedance characteristic [45]. The electrochemically deposited iridium oxide coating is an emerging material to decrease the impedance. It shows good adhesion, on platinum notably, and

good stability properties in saline solution [12, 46, 47]. Another new electrodes material consists of titanium nitride deposited in thin film by a sputtering technique and showing a porous surface texture [48]. The sizes of the microelectrodes are usually about 100 μm^2, the recorded extracellular potentials are typically about several 100 µV with a frequency bandwidth from 100 Hz to 10 kHz.

An alternative method for the detection of extracellular potentials consists in using the gate oxide of a field effect transistor [49, 50]. In this case, the probe material is silicon dioxide or silicon nitride instead of metal. Another method uses voltage sensitive dies and optical recording [51]. An increasing interest appears for the measurements of parameters other than the potentials. The pH changes produced by the metabolism of the culture were measured by using light addressable potentiometric sensor on a device called microphysiometer [52, 53]. The cells morphology and their adhesion on the substrate can be studied by using conductivity measurements on interdigitated array [54]. A great variety of sensors were integrated on the same chip to obtain information on several parameters of the physiological activity of the culture [55]. The analyse of the perfusion's outlet can also be performed [56]. The cultured neurons can act as sensors by themselves. Their responses to bioactive agent are measured and can be quantified [57, 58, 59].

It should be noted that none of the so far described MEAs has three dimensional electrodes. This means that these electrodes detect the signal emitted above the plane of the substrate only through an electrically passive layer. Of course, the three dimensional electrodes are justified only if the device is applied to culture with thick slice of tissue. This aspect has nevertheless been described in a general way [60] and in *in vivo* implants (see above). Theoretical analysis were also undertaken to discover the effect of the distance between the neuron and the electrode and to demonstrate a significant attenuation of the signal on a distance in the order of some tens of micrometers [61, 62].

1.2. Comparison with classical microelectrodea

The classical electrodes, which are used to measure the neuron's potentials can be of different types. One of them is simply a fine passivated wire electrode. Another one consists of a wire inserted in glass micro pipette filled with a saline solution. The contact between the wire and the electrolyte can be ohmic if this wire is in Ag/AgCl. If the inserted wire is metallic, a low impedance is obtained due to its size. The micro pipette is also used to measure potentials by using the patch clamp method. This method enables to measure current trough a small part of the neurons' membrane. It consists of approaching a fine glass micro pipette with a fire polished tip to the cell membrane and to apply suction to form a seal between the inner face of the pipette and the membrane. The patch of the membrane can be extracted and both sides of it can be reached. Another measurement technique has to be mentioned: the optical recording. The optical recording uses different dyes and the changes of the light absorption can be measured by a photodetector. This technique has the advantage to avoid mechanical injury to the tissue.

The micro pipettes are fabricated by the expansion of a glass tube locally heated. By this method, a very small aperture is formed, down to 30 nm for the smallest ones, like the one shown in fig. 1.1. With its small size, the classical microelectrode can be inserted either inside the neurons to measure the intracellular potentials or outside for the extracellular potentials like explained in paragraph 2.3. These microelectrodes can be used for *in vivo* and *in vitro* applications with a minimum of damages in the tissue. They are mounted on micro-manipulator in order to be placed with a great precision at a point of measurement. To illustrate this set up, the fig. 1.2. shows a commercially available equipment for electrophysiology. This operation requires time and ability of the experimenter, especially for not damaging the cells. The micro-

Fig. 1.1. Classical glass microelectrode.

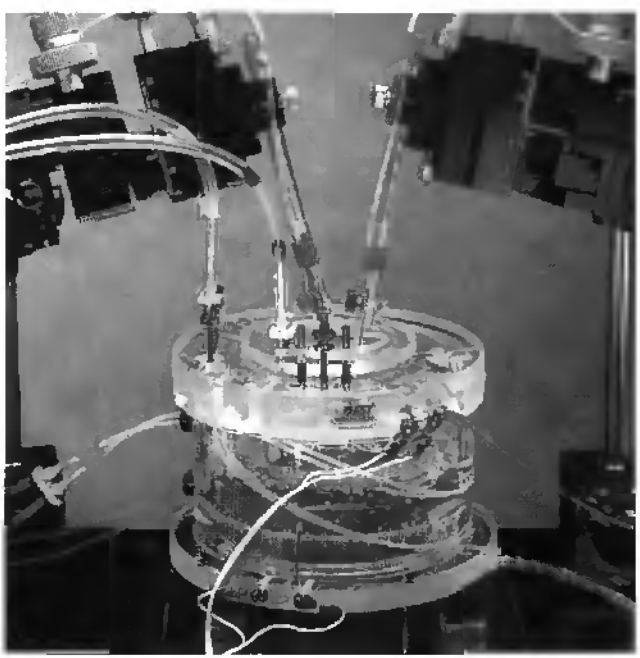

Fig. 1.2. Commercially available equipment for electrophysiology with two microelectrodes (fine science tools inc.).

manipulators, one for each electrode, take a lot of place and therefore, only few electrodes can be used simultaneously, the maximum being four. After the measurements, the culture has to be put back into the incubator. For each experiment, the electrodes have to be set up again.

The microelectrodes, which have a size of typically 10 µm, are much bigger than classical glass electrode. As a consequence, the points of measurements are less localised. Since the MEAs are made with metal, their coupling with the extracellular fluids is not ohmic as explained in paragraph 4.2. Nevertheless, this contact can be improved by lowering the impedance of the electrodes. The positions of the array of electrodes cannot be controlled with the same accuracy than the glass pipettes. This fact is not problematic for the measurements on dissociated culture in which the cells cover the whole surface. For slice cultures, the adjustment is performed when the tissue is deposited on the substrate. That is why, the microelectrodes are distributed in a certain area of the culture. Since they are more numerous, some of them are in a good position for the measurements. A sufficient density of electrodes and a design adapted for the culture which is studied can enhance this aspect. After that the neurons are deposited on the MEA, the disposition of the electrodes remains the same during the whole culturing time. The device and the tissue are stored together in the incubator in order to keep the cells alive and this stack is inserted in the measurement set-up only when an experiment has to be performed. So, the evolution of the tissue can be observed in an easier and a faster way, and thus, a great number of cultures can be performed at the same time. The advantages and drawbacks of the microelectrode arrays, compared with the classical electrodes, are summarised as follow:

Advantages of the MEA:

- permanent location
- numerous electrodes
- easy to handle

Drawbacks of the MEA:

bigger size of the electrodes

control of the placement

less efficient electrical coupling

In conclusion, the MEA represents an interesting alternative to the classical electrodes, especially for long term investigations and for the study of the network formed by the neurons. It is also possible to combine both classical and microfabricated electrodes in the same experiment. The facility of use of the MEA helps the neurophysiologists by increasing the number of experiments which can be performed.

1.3. Objectives and outline

The objective of this work consists of the realisation of microelectrode arrays suited to the culture of neurons and enabling to measure extracellularly their activity. The basic structure of these devices consists of an array of metal electrodes embedded on a passivated substrate. These electrodes are covered by a top insulation layer with small open area located on each electrode and a contact pad to connect this electrode to the measurement set-up.

Two features have to be included in this device: it should be adapted to organotypic culture by interface and the electrical coupling with the neuroactive cells has to be enhanced. As it will be explained in this work, these goals can be achieved by fabricating respectively:

a perforated substrate

three dimensional microelectrodes

The device is schematically shown in the fig. 1.3.

Chapter 2 will explain the requirements of the microfabricated device. The specificity of the organotypic culture by interface will be exposed, together with the conditions in which this culture can be kept alive for a long time. The

morphology of the rat's hippocampus which will be used to test the MEAs will be described. Some explanations about the extracellular measurements will highlight the advantages of the three dimensional electrodes.

Chapter 3 will describe the fabrication processes of the devices by using the facilities available in the Institute of Microtechnology, University of Neuchâtel. Explanations will be given about the technical solutions which were found to fulfil the above requirements.

Chapter 4 will expose the electrical characterisations of the MEA. The tests of viability for a long term organotypic culture by interface will be shown. The integration of the device in a measurement set-up for electrophysiology will be described as well as the results obtained with the rats' hippocampus.

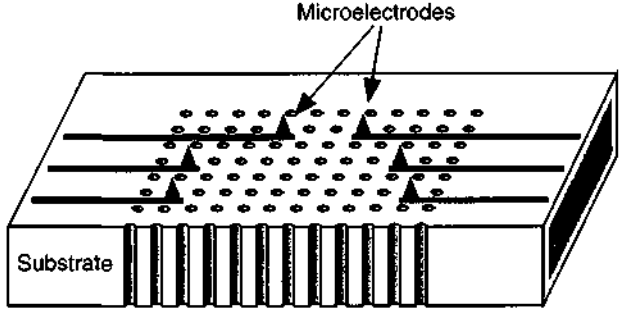

Fig. 1.3. Scheme of the device.

Referencee

1 D. A. Stenger and T. M. McKenna "Enabling technologies for cultured neural networks" academic press, San Diego (USA), 1994

2 http://www.caltech.edu/~pinelab/multielectrodeRefs.html

3 http://www.ee.surrey.ac.uk/Personal/D.Banks/bibs.html

4 K. Najafi "Solid-state microsensors for cortical nerve recordings" IEEE engineering in medicine and biology, 1994, p. 375-387

5 G. T. A. Kovacs, C. W. Storment, and J. M. Rosen "Regeneration microelectrode array for peripheral nerve recording and stimulation" IEEE transactions on biomedical engineering, vol. 39, 1992, p.893-902

6 S. A. Boppart, B. C. Wheeler, and C. S. Wallace "A flexible perforated microelectrode array for extended neural recordings" IEEE transactions on biomedical engineering, vol. 39, 1992, p. 37-42

7 J. F. Hetke, J. L. Lund, K. Najafi, K. D. Wise, and D. J. Anderson "Silicon ribbon cables for chronically implantable microelectrode arrays" IEEE transactions on biomedical engineering, vol. 41, 1994, p.314-321

8 N. A. Blum, B. G. Carkhuff, H. K. Charles, R. L. Edwards, and A. Meyer "Multisite microprobes for neural recordings" IEEE transactions on biomedical engineering, vol. 38, 1991, p. 68-74

9 M. O. Heuschkel, P. Renaud, J. Streit, B. Buisson, and D. Bertrand "Design of multielectrode arrays for long-term stimulation and recordings of neurons in culture" Abstracts of international meeting on substrate-integrated microelectrode arrays, Reutlingen (Germany), 1998, p. 9

10 M. O. Heuschkel, L. Guérin, B. Buisson, D. Bertrand, and P. Renaud "Microfluidic system for perfusion of solutions to neurons in a network"

11th. European Conf. on Solid-State Transducers, Eurosensors XI, Warsaw (Poland), 1997, p. 349-352

11 D. J. Edell "A peripheral nerve information transducer for amputees: long-term multichannel recordings from rabbit peripheral nerves" IEEE transactions on biomedical engineering, vol. 33, 1986, p.203-214

12 T. Akin, K. Najafi, R. H. Smoke, and R. M. Bradley "A micromachined silicon sieve electrode for nerve regeneration applications" IEEE transactions on biomedical engineering, vol. 41, 1994, p. 305-313

13 G. T. A. Kovacs, C. W. Storment, M. Halks-Miller, C. R. Belczynski, C. C. Della Santina, E. R. Lewis, and N. I. Maluf "Silicon-substrate microelectrode arrays for parallel recording of neural activity in peripheral and cranial nerves" IEEE transactions on biomedical engineering, vol. 41, 1994, p.567-577

14 J.-U. Meyer, H. Beutel, E. Valderrama, E. Cabruja, P. Aebischer, G. Soldani, and P. Dario "Perforated silicon dices with integrated nerve guidance channels for interfacing peripheral nerves" Proceedings of IEEE Micro Electro Mechanical Systems, Amsterdam, 1995, p.358-361

15 J. J. Mastrototaro, H. Z. Massoud, T. C. Pilkington, and R. E. Ideker "Rigid and flexible thin-film multielectrode arrays for transmural cardiac recording" IEEE transactions on biomedical engineering, vol. 39, 1992, p. 271-279

16 W. L. C. Rutten, H. J. Van Wier and H. M. Put "Sensivity and selectivity of intraneural stimulation using a silicon electrode array" IEEE transactions on biomedical engineering, vol. 38, 1991, p. 192-198

17 A. B. Frazier, D. P. O'Brien, and M. G. Allen "Two dimensional metallic microelectrode arrays for extracellular stimulation and recording of neurons" Proceedings of IEEE Micro Electro Mechanical Systems, Fort Lauderdale 1993, p.195-200

18 A. C. Hoogerwerf and K. D. Wise "A three-dimensional microelectrode array for chronic neural recording" IEEE transactions on biomedical engineering, vol. 41, 1994, p.1136-1146

19 P. K. Campbell, K. E. Jones, R. J. Huber, K. W. Horch, and R. A. Normann "A silicon-based, three-dimensional neural interface: manufacturing processes for an intracortical electrode array" IEEE transactions on biomedical engineering, vol. 38, 1991, p. 758-768

20 R. A. Normann "Visual neuroprosthetics-Functional vision for the blind" IEEE engineering in medicine and biology, 1995, p. 77-83

21 D. J. Edell, V. Van Toi, V. M. McNeil, and L. D. Clark "Factors influencing the biocompatibility of insertable silicon microshafts in cerebral cortex" IEEE transactions on biomedical engineering, vol. 39, 1992, p.635-643

22 C. A. Thomas, P. A. Springer, G. E. Loeb, Y. Berwald-Netter, and L. M. Okun "A miniature microelectrode array to monitor the bioelectric activity of cultured cells" Experimental cell research, vol. 74, 1972, p. 61-66

23 G. W. Gross "Simultaneous single unit recording *in vitro* with a photoetched laser deinsulated gold multimicroelectrode surface" IEEE transactions on biomedical engineering, vol. 26, 1979, p. 273-279

24 J. Pine "Recording action potentials from cultured neurones with extracellular microcircuit electrodes" Journal of neuroscience methods, vol. 2 ,1980, p. 19-31

25 D. A. Israel, W. H. Barry, D. J. Edell, and R. G. Mark"An array of microelectrodes to stimulate and record from cardiac cells in culture" American Journal of physiology, vol. 247, 1994, p. H669-H674

26 G. W. Gross, W. Y. Wen and J, W. Lin "Transparent indium-tin oxide electrode patterns for extracellular, multisite recording in neuronal cultures" Journal of neuroscience methods, vol. 15, 1985, p. 243-252

27 P. Connolly, P. Clark, A. S. G. Curtis, J. A. T. Dow, and C. D. W. Wilkinson "An extracellular microelectrode array for monitoring

electrogenic cells in culture" Biosensors & Bioelectronics, vol. 5, 1990 p. 223-234

28 J. L. Novak and B. C. Wheeler "Multisite hippocampal slice recording and stimulation using a 32 element microelectrode array" Journal of neuroscience methods, vol. 23, 1988, p. 149-159

29 J. A. T. Dow, P. Clark, P. Connolly, A. S. G. Curtis, and C. D. W. Wilkinson " Novel methods for guidance and monitoring of single cells and simple networks in culture" Journal of Cell Science Suppl., vol. 8, 1987, p. 55-79

30 Y. Jimbo and A. Kawana "Electrical stimulation and recording from cultured neurons using a planar electrode array" Bioelectrochemistry and Bioenergetics, vol. 29, 1992, p. 193-204

31 J. M. Corey, B. C. Wheeler, and G. J. Brewer "Micrometer resolution silane based patterning of hippocampal neurons: critical variables in photoresist and laser ablation processes for substrate fabrication" IEEE transactions on biomedical engineering, vol. 43, 1996, p. 944-955

32 M. Matsuzawa, P. Liesi, W. Knoll "Chemically modifying glass surfaces to study substratum-guided neurite outgrowth in culture" Journal of neuroscience methods, vol. 69, 1996, p. 189-196

33 S. A. Makohliso, L. Giovangrandi, D. Léonard, H. J. Mathieu, M. Ilegems, P. Aebischer "Application of teflon-AF® thin film for bio-patterning of neural cell adhesion" Biosensors & Bioelectronics, vol. 13, 1998, p. 1227-1235

34 S. Tatic-Lucic, J. A. Wright, Y.-C. Tai, and J. Pine " Silicon cultured-neuron prosthetic devices for In Vivo and In Vitro studies " Sensors and Actuators B, vol 43, 1997, p. 105-109

35 G. Fuhr, T. Schnelle, T. Müller, H. Glasser, T. Lisec and B. Wagner "Positioning and manipulation of cells and microparticles using miniaturized

electric field traps and travelling waves" Sensors and Materials, vol. 7, 1995, p. 131-146

36 G. W. Gross and F. U. Schwalm "A close flow chamber for long-term multichannel recording and optical monitoring" Journal of neuroscience methods, vol. 52, 1994, p. 73-85

37 L. Stoppini, S. Duport, and P. Corrèges "A new extracellular multirecording system for electrophysiological studies: application to hippocampal organotypic cultures" Journal of neuroscience methods, vol. 72, 1997, p. 23-33

38 M. Bove, M. Grattarola, and G. Verreschi "*In Vitro* 2-D networks of neurons characterized by processing the signals recorded with a planar microtransducer array" IEEE transactions on biomedical engineering, vol. 44, 1997, p. 964-977

39 W. Nisch, J. Böck, U. Egert, H. Hämmerle, and A. Mohr "A thin film microelectrode array for monitoring extracellular neuronal activity *in vitro*" Biosensors & Bioelectronics, vol. 9, 1994, p. 737-741

40 H. Hämmerle, U. Egert, A. Mohr, and W. Nisch "Extracellular recording in neuronal networks with substrate integrated microelectrode arrays" Biosensors & Bioelectronics, vol. 9, 1994, p. 691-696

41 E. Maeda, H. P. C. Robinson and A. Kawana "The mechanisms of generation and propagation of synchronized bursting in developing network of cortical neurons" The journal of neuroscience, vol. 15, 1995, p. 6834-6845

42 C. Leibrock, T. Knott, H. Hämmerle, and T. Müller "Intrinsic proprieties of hippocampal cultures recorded with planar microelectrode arrays" Abstracts of international meeting on substrate-integrated microelectrode arrays, Reutlingen (Germany), 1998, p. 24

43 H. Sugihara, H. Oka, R. Ogawa, K. Shimono, and M. Taketani "In vitro network physiology comes of age" Abstracts of international meeting on

substrate-integrated microelectrode arrays, Reutlingen (Germany), 1998, p. 48

44 S. A. Boppart, B. C. Wheeler, and C. S. Wallace "A flexible perforated microelectrode array for extended neural recordings" IEEE transactions on biomedical engineering, vol. 39, 1992, p. 37-42

45 M. Hyland, J. A. McLaughlin, D. -M. Zhou and E. T. McAdams "Surface modification of thin film gold electrodes for improved *in vivo* preformance" Analyst, vol. 121, 1996, p. 705-709

46 R. Fröhlich, A. Rzany, J. Riedmüller, A. Bolz, and M. Schaldach "Electroactive coating of stimulating electrodes" Journal of materials science: materials in medicine, vol. 7, 1996, p. 393-397

47 T. M. Silva , J. Rito, M. G. S. Ferreira, I. Fonseca,, and K. Watkins "Electrochemical response of iridium oxide for implanted neural stimulating electrodes" Journal of materials science: materials in medicine, vol. 7, 1996, p. 261-264

48 M. Stelzle, M. Dürr, V. Bucher, B. Brunner, and W. Nisch "Improvement and design of micro-electrode arrays for applications in pharmaceutical R&D" Abstracts of international meeting on substrate-integrated microelectrode arrays, Reutlingen (Germany), 1998, p. 10

49 P. Fromherz, A. Offenhäusser, T. Vetter, J. Weis "A neuron-silicon junction: a retizus cell of the leech on an insulated-gate field-effect transistor" Science, vol. 252, 1991, p. 1290-1293

50 A. Offenhäuser, C. Sprössler, M. Matsuzawa and W. Knoll "Field-effect transistor array for monitoring electrical activity from mammalian neurons in culture" Biosensors & Bioelectronics, vol. 12, 1997, p. 819-826

51 T. D. Parsons, D. Kleinfeld, F. Raccuia-Behling, and B. M. Salzberg "Optical recording of the electrical activity of synaptically interacting *Aplysia* neurons in culture using potentiometric probes" Biophysical journal, vol. 56, 1989, p. 213-221

52 J. C. Owicki and J. W. Parce "Bioassays with a microphysiometer" Nature, vol. 344, 1990, p. 271-272

53 J. C. Owicki and J. W. Parce "Biosensors based on the energy metabolism of living cells: the physical chemistry and cell biology of extracellular acidification" Biosensors & Bioelectronics, vol. 7, 1992, p. 255-272

54 C. R. Keese and I. Giaever "A Biosensor that monitors cell morphology with electrical fields" IEEE engineering in medicine and biology, 1994, p. 402-408

55 B. Wolf, M. Brischwein, W. Baumann, R. Ehret, and M. Kraus "Monitoring of cellular signalling and metabolism with modular sensor technique: the physiocontrol-microsystem (PCM®)" Biosensors and Bioelectronics, vol. 13, 1998, p. 501-509

56 Y.-M. Liu, T. Moroz, and J. V. Sweedler "Monitoring cellular release with dynamic channel electrophoresis" Analytical Chemistry, vol 71, 1999, p. 28-33

57 G. W. Gross, B. K. Rhoades, H. M. E. Azzazy, and M.-C. Wu "The use of neuronal networks on multielectrode arrays as biosensors" The journal of neuroscience, vol. 6, 1986, p. 1583-1592

58 G. W. Gross, A. Harsch, B. K. Rhoades, and W. Göpel "Odor, drug and toxin analysis with neuronal network *in vitro*: extracellular array recording of network responses" Biosensors & Bioelectronics, vol. 12, 1997, p. 373-393

59 D. A. Borkholder, B. D. DeBusschere, and T. A. Kovacs "An approach to the classification of ouknown biological agents with cell based sensors" Solid-State Sensor and Actuator Workshop, Hilton Head Island (USA), 1998, p. 178-182

60 C. L. Byers, J. H. Schulman, and D. I. Whitmoyer "Method of making an electrode array" US patent n° 4 837 049, June 1989

61 R. Lind, P. Connolly, C. D. W. Wilkinson, and R. D. Thomson "Finite-element analysis applied to extracellular microelectrode design" Sensors and Actuators B, vol. 3, 1991, p. 23-30

62 M. Bove, M Grattarola, and S. Martinoia "Coupling of networks of neurones to substrate planar microtransducers - A Review" Neurobiology, vol. 20, 1996, p. 251-264

2. Electrophysiological aspects

Some characteristics of the organotypic culture by interface for which the devices have to be adapted will be explained. A description of the rat hippocampus which will be cultured on these devices will be given. Aspects of extracellular potentials measurements will be approached. The basic biological phenomena which produce them are described in the annexe. A more detailed analysis of these subjects is given in [1, 2, 3, 4, 5, 6].

2.1. Organotypic culturaa

Although slightly less representative compared with *in vivo* experiments, the cultures represent an interesting alternative with several advantages. The number of sacrificed animals is lowered because a single one can produce several explants. With the *in vitro* method, experiments on tissues coming from human beings can also be considered. An *in vitro* culture should represent the *in vivo* organ as closely as possible. The degree of similarity can be very different according to the type of culture used. The main aspects in order to evaluate a culture consist in its cells arrangement and in the conservation of the interactions between these cells. The experimental difficulties are increased with the complexity of the cells structure. The choice of the culture used should thus be adapted to the research undertaken. A description of these cultures is given in [7]. As an example, a dissociated culture embedded on a silicon chip with platinum microelectrode is shown in fig 2.1. In this case the neurons are separated and distributed on the substrate. A culture is considered as organotypic if the morphology, the synaptic circuitry, the neurotransmitter receptor distribution and the electrophysiology are similar to these *in vivo*. Therefore this culture consists of a slice of tissue several hundred µm thick.

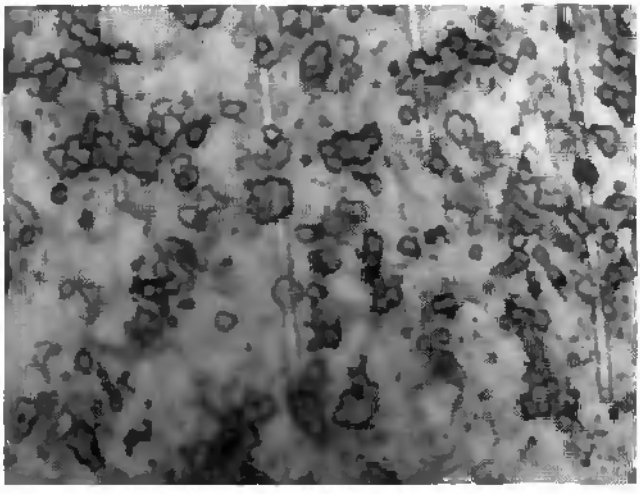

Fig. 2.1. Dissociated culture on a silicon chip (photography performed by the Prof. Grattarola's group).

Three aspects are important for a good culture survival: the substrate, the access to the nutritive medium, and the gas exchanges. First of all, the materials used have to be biocompatible which implies that they should show no toxicity. In order to survive, the cells need a nutritive influx, an absorption of oxygen and a release of carbon dioxide. The cells' membrane is easily accessible in a dissociated culture and exchanges can take place. This goal is more difficult to reach for as thick slice cultures like organotypic's ones. Two methods are currently used:

1) the Gähwiler or roller drum method or immerse culture [8, 9, 10]

2) the Stoppini method or culture by interface or insert culture [11, 12, 13].

The roller drum method consists in attaching an explant of 400 µm thick on a glass coverslip by means of a clot prepared with chicken plasma. The coverslip is then put into a plastic test tube containing adequate medium and placed on a roller drum which rotates at a specific speed and with appropriate angle so that the slice is alternatively covered by the medium and the air.

In the organotypic culture by interface, the explant is placed on a porous membrane at the interface between air and medium. A scheme of this set up is shown in fig. 2.2. The bottom side of the slice has a contact with the medium, through the substrate. On the upper side, a thin film of medium covers the slice avoiding its drying. Since the gas exchange takes place by diffusion and mainly at the top side, this film should not be too thick. This method does not require any adhesion layer like plasma clot, collagen, laminin or fibronectin and avoids thus any interaction of these products with the neurons. The tissue is cut in slices 400 μm thick and simply laid down on small disk of porous Millicell-CM membrane from Millipore® and placed in a petri dish with the medium. This set-up is stored in an incubator with 5% CO_2 at 36° [11]. This temperature can be decreased after the first week down to 33° in order to make the tissue survive for a longer time [14].

The Stoppini method is well adapted for a substrate embedded MEA. The signal detection for continuous recording is easier if the set up does not have to move regularly as for the roller drum method and no isolating adhesion material is required to fix the slice on the substrate where the electrodes are embedded.

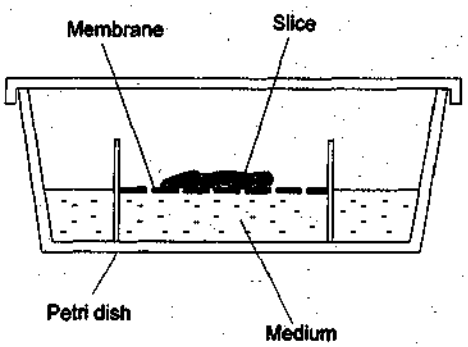

Fig. 2.2. Scheme of the set-up of the organotypic culture by interface (modified from [11]).

Culture of cells are successful only with a young tissue. This can be understood owing to the property of these cells which consists of adapting themselves easily to a new environment. In order to study a tissue with enough maturity and differentiation between the cells, the culture has to survive for several weeks. 3 months of survival were obtained with the Stoppini method described here with hippocampus of seven days old Wistar rats [12]. However a culture of 3-5 weeks is considered as sufficiently mature for most experimental purposes. During this time the slice recovers from the injuries made during its preparation and a reorganisation of the connections occurs. Electrical stimulations enhance also new synaptic transmissions between the neurons. A slice cut in two part and placed aside with a small gap can be reformed by the sprouting of the connections. This property can be used by culturing together several tissues in a co-culture, also with tissues coming from different parts of the brain. A lot of organotypic experiments were made with hippocampal slices of rats. This part of the brain is described in the next paragraph. Fig 2.3. shows a cross section of this tissue after two weeks of culture by using the Stoppini method. The thickness of the slice is reduced down to 150 μm and three layers can be identified. The upper part is constituted by the fibres, axons and dendrites. In the middle part, the somas of the neurons can be seen. The lower part, which is in contact with the porous substrate is formed by glial cells. These cells are involved in the ions exchanges with the medium and the neurons and act as support. This 50 μm thick layer isolates the electrodes from the signal produced in the soma layer. The histology of the cultured slices is different according to the method used. By the Gähwiler, a single layer of neurons is formed in the centre of the slice. Hence, during electrophysiological experiment, less neurons can contribute to the measured signal and the three dimensional aspect of the network formed between the neurons is less complex. On the other hand the observation through a microscope of a slice cultured with this method is easier because all the neurons can be well distinguished.

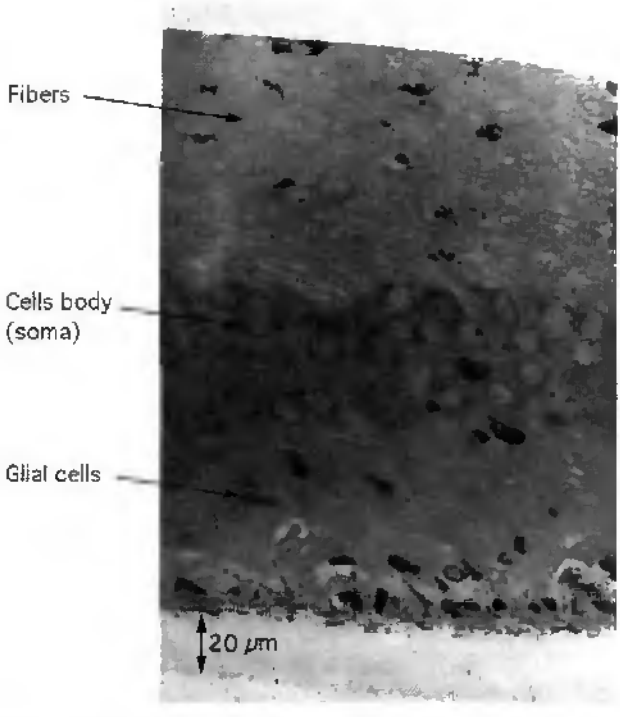

Fig. 2.3. Cross section of an hippocampal slice after two weeks of the organotypic culture by interface (photography performed by Dr. Stoppini).

In both methods, an electrically passive layer of glial cells subsists on the substrate. In order that the electrodes are closer to the soma of the cells, three dimensional electrodes which can penetrate in this layer will be fabricated.

2.2. Rat's hippocampus

The hippocampus is placed in the medial temporal lobe shown in fig 2.4. This part of the brain play an important role in certain aspects of learning and memory, especially the memory for facts and events called declarative

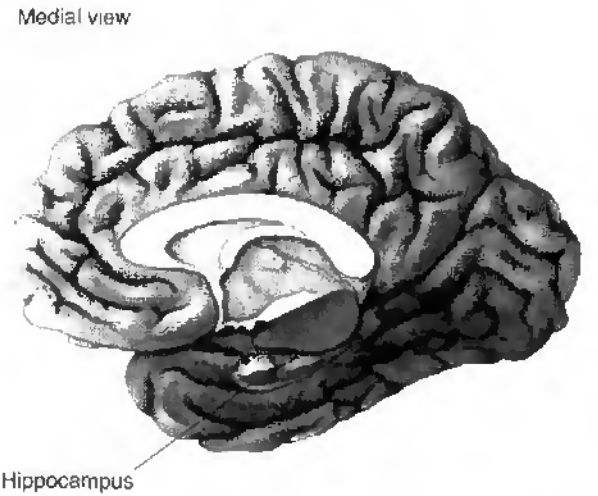

Fig. 2.4. Position of the hippocampus in human brain (modified from [5]).

memory. The hippocampus is involved in making associations between the current situation and previous ones that the subject has already lived. For that reason, it receives inputs from parts of the sensory systems. Its morphological shape is a curved cylinder which can be cut in cross slices. Because of a highly regular organisation, each slice shows a similar structure. Since much of synaptic transmissions occur in this transverse direction, a slice keeps intact a great part of the connected fibres. A lot of neurotransmitters are present in the hippocampus. The main ones are the glutamate as excitatory transmitters and the GABA as inhibitory. This lamellar structure is very convenient for making many identical cultures; up to 16 with a single 7 days old rat. This experimental reproducibility and the interesting functions realised by the hippocampus make it one of the most studied parts of the brain, in particular in cultures. A plan of an hippocampus slice is shown in fig 2.5. Its main components consist of two types of neurons: granule cells in the dentate gyrus and the pyramidal neurons in a region divided into two parts CA1 and CA3.

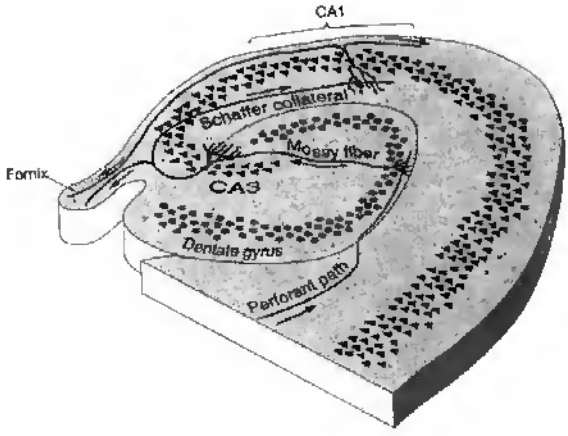

Fig. 2.5. Scheme of an hippocampus slice (from [5]).

These two types of neurons form two lines folded into each other. The hippocampus receives informations through axons called perforant path. They are mainly connected to the dentate gyrus. From there, the Mossy fibers reach the pyramidal cells up to in the CA3 area. One of the branches of the axons starting from the CA3 part, the Schaffer collateral, forms synapses towards the next region, the CA1. The other branch as well as the axons starting form CA1 part have their targets outside of the hippocampus.

This simplified scheme highlights the unidirectional aspect of the main connections allowing several types of experiments to be performed. A typical one is the following: an electrical stimulation is sent in the CA3 region by the mean of a microelectrode. This stimulation is transmitted by the Schaffer collateral to the CA1 region where the evoked response is recorded by another microelectrode. Such experiment emphases several effects like, for instance, long term potentiation (LTP). If a depolarisation and the activation of a type of glutamate receptor occur at the same time, the properties of the neuron change for a long time by giving a stronger excitatory postsynapitc potential (EPSP) than initially. This phenomenon of LTP can be induced by an external high

frequency stimulation. The opposite, long term depression (LTD) can also be produced by applying an external low frequency stimulation. Linked to other types of studies, the changes in effectiveness of synaptic transmission are considered to be the basis processes for learning and memory.

2.3. Extracellular potentials

The methods used to measure the potential changes generated by the neuron activity can be divided into two types: intracellular and extracellular. Both use the classical microelectrodes described in paragraph 1.2. For the intracellular recordings, the tip of the microelectrode is inserted inside the cell, introducing some damages to it. The electrical potential generated through the membrane is recorded between the interior of the cell by the microelectrode and the extracellular fluid by the reference electrode. The extracellular recordings are made by measuring between the microelectrode placed close to the cell body or the axon, and the reference electrode. Both cases are illustrated in fig 2.6. In the case of the MEA, the extracellular potentials are measured by a metallic electrode.

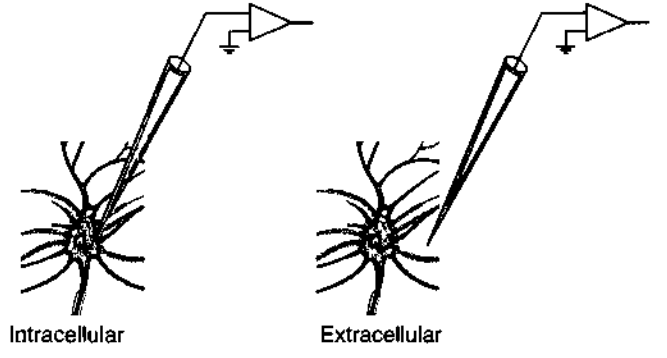

Fig. 2.6. Schemes of intracellular and extracellular measurements (modified from [1]).

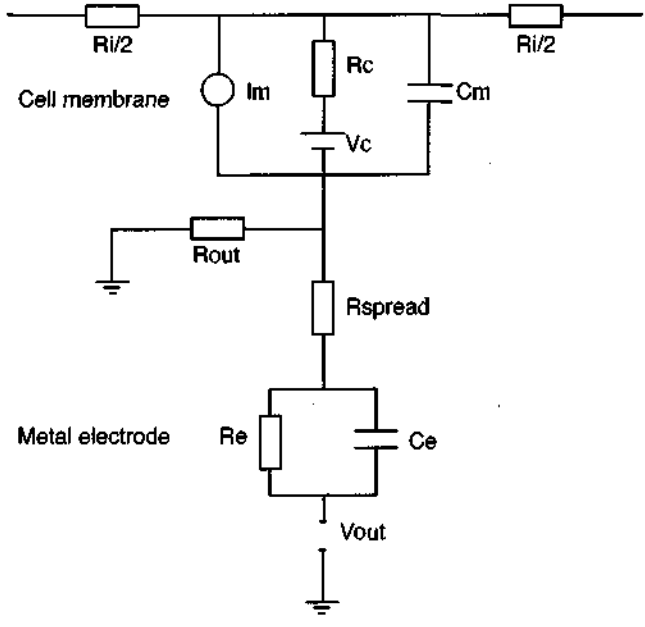

Fig 2.7. Equivalent circuit of the coupling between the cell membrane and the metal electrode (modified from [15]).

By using the equivalent circuit of a membrane patch of a cell given in paragraph A.1. and the model of a metal electrode-electrolyte interface given in the paragraph 4.2., an equivalent circuit, shown in fig. 2.7., of the coupling between the neuron and the electrode can be obtained. A part of the current Im reaches the microelectrode through the resistance Rspread and another part goes outside the measurement area through Rout. Thus, to obtain a good coupling with the electrode, Rspread which depends mainly of the distance electrode-neuron should be as small as possible [15].

If a microelectrode is placed sufficiently close to the cell, the activity of a single neuron can be recorded. Another approach in electrophysiology is the recordings of the potential differences generated by a group of neurons and measured at some distance from them. They are called field potentials and are generated by both the synaptic and the action potentials. This kind of potentials

can be measured by the MEA. Depolarisation on the membrane induces potential differences between one part of the neuron and the other and thus a current flows through the extracellular space as illustrated on the fig 2.8. The depolarisation takes place at a point A and is called sink because it consists in an inward current Im. Since the current flows inside, charges must leave the cell. One outward path is a point B called source which can be defined, among the multitude available, as the point where the current flows out after travelling through the intracellular space (Rint). The current returns to A to close the loop through the extracellular fluid (Rext) but also to a reference electrode located at some distance. The fig 2.9. illustrates the electrical fields produced by an excitatory synapse placed on a dendrite and shows two extracellular potential measurements: negative potential near the sink and positive potential around the source. For an inhibitory synapse placed on a dendrite, the current flow is inverted. During an EPSP the soma acts as a source. An extracellular measurement in this position, which is the position of the MEA, will show a positive recording. If an action potential is initiated, the big surface of the soma will depolarise, letting the current go inside and results

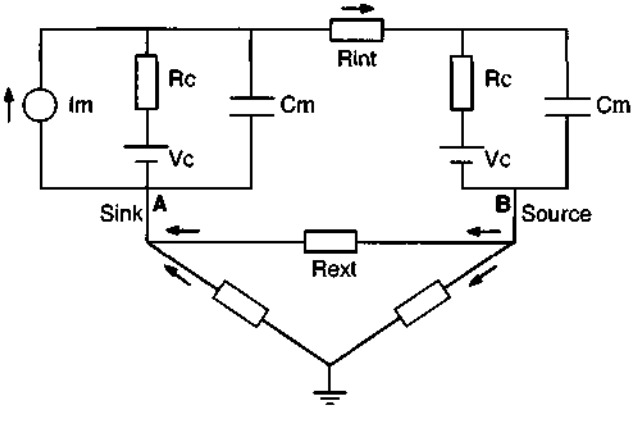

Fig 2.8. Charges movements between two points of the membrane at a different potential (modified from [4]).

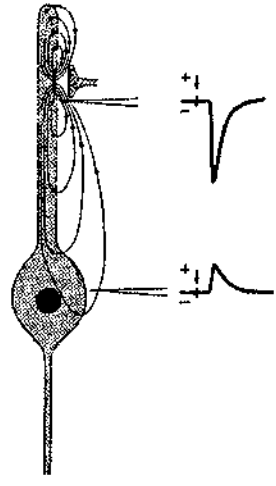

Fig. 2.9. electrical fields around an excitatory synapse (modified from [4]).

in a negative spike, the dendrites becoming the source. The action potential still propagates and the soma acts as a source again. As a consequence, the extracellular measurement near the soma is theoretically a triphasic positive - negative - positive wave.

A measurement in the extracellular space does not measure the contribution a single neuron but of several. The most important aspect, as far as the amplitude of the recording is concerned, is the number and the arrangement of the neurons around the electrode. The contribution of one neuron can be cancelled by another one of an opposite orientation. The radial disposition of the neurons is referred to as a closed field. Either the somas or the dendrites are located in the centre and the other part in the periphery. If all the cells are activated, the potential is zero outside the formed sphere. When all neurons are oriented in the same direction: the somas on one side, the dendrites on the another side, they are designated as open field. The combination of both is the open-closed field. The hippocampus cells are typically arranged as an open field.

The experiment commonly made on hippocampus, consists of measuring the response in the CA1 region after a stimulation of the Schaffer collateral in the CA3 region. The extracellular electrode will measure the EPSP's in the dendrites of all cells around it and will be called population EPSP. If they are sufficiently strong, the action potentials will be induced in the somas and will be called population spike. Due to the open field arrangement, the measured field potential corresponds to the addition of all the synchronous activity of the group of cells near the electrode which can be interpreted as the amplified averaged response of a single cell.

The stimulation pulse produces a big artefact in the measurements, disturbing the cells' signals. If the stimulation electrode is more distant, the artefact and the population spikes are more separate because of the longer travelling time of the action potential in the presynaptic axon's cells. Another difficulty of these measurements is the time scale of the recorded waves which is close to the 50 Hz noise, requiring a good shielding.

These considerations show the importance of the geometrical arrangement neurons-electrode and highlights the advantage of having a shorter distance between them by using, in this work, three dimensional electrodes.

References

1 J. G. N. Nicholls, A. R. Martin, and B. G. Wallace "From Neuron to Brain", Sinauer associates, Sunderland (USA), 1992

2 G. M. Shephard "The Synaptic Organisation of the Brain" Oxford University press, New York (USA), 1990

3 E. R. Kandel, J. H. Schwrtz, T. M. Jessell, "Principles of neural science", Appleton & Lange, East Norwalk (USA), 1991

4 J. I. Hubbard, R. Llinas, and D. M. Quastel "Electrophysiological analysis of synaptic transmission", Edward Arnold publishers LTD, London, 1969

5 M. F. Bear, B. W. Connors, and M. A. Paradiso "Neuroscience: exploring the brain", Williams & Wilkins, Baltimore (USA), 1996

6 D. A. Stenger and T. M. McKenna "Enabling technologies for cultured neural networks" academic press, San Diego (USA), 1994

7 A. A. Boulton, G. B. Baker, and W. Walz "Neuromethods 23: Practical cell cuture techniques", Humana press, Totowa (USA), 1992

8 B. H. Gähwiler "Organotypic monolayer cultures of nervous tissue", Journal of neuroscience methods, vol. 4, 1981, p. 329-342

9 J. Zimmer and B. H. Gähwiler "Cellular and connective organization of slice cultures of the rat hippocampus and fascia dentata", The journal of comparative neurology, vol. 228, 1983, p. 432-446

10 B. H. Gähwiler "Organotypic cultures of neural tissue", Trends neurol. sci., vol 11, 1988, no 11, p. 484-489

11 L. Stoppini, P.-A. Buchs, and D. Muller "A simple method for organotypic cultures of nervous tissue", Journal of neuroscience methods, vol 37, 1991, p. 173-182

12 L. Stoppini, S. Duport and P. Corrèges "A new extracelluler multirecording system for electrophysiological studies: application to hippocampal organotypic cultures", Journal of neuroscience methods, vol 72, 1997, p. 23-33

13 B. A. Bahr, "Mini-review: long-term hippocampal slices: a model system for investigating synaptic mechanisms and pathologic processes", Journal of neuroscience research, vol. 42, 1995, p. 294-305

14 P. Thiébaud, N.F. de Rooij, M. Koudelka-Hep, and L. Stoppini "Microelectrode arrays for electrophysiological monitoring of hippocampal organotypic slice cultures" IEEE transactions on biomedical engineering, vol. 44, 1997, p. 1159-1163

15 M. Grattarola and G. Massobrio "Bioelectronics handbook: MOSFETs, biosensors, & neurons" McGraw-Hill, New York (USA), 1998

3. Fabrication processes

Fabrication of several microelectrode arrays (MEA), suitable for electrophysiological measurements will be described in this chapter. The choice of the technologies, as far as the biological and the technical requirements are concerned, will also be explained. The MEA have to fit to the morphology of the slice which has, at the bottom, an electrically passive layer, and also to ensure good survival conditions which are required by the organotypic cultures by interface. The literature gives more detailed information about these technologies [1, 2, 3, 4, 5].

3.1. Microelectrode array on a transparent substrate

A transparent device allows the observation of the culture during the experiment using a microscope with a bottom side illumination. For this reason, a glass substrate will be used. The electrodes embedded on it, will be in platinum, forming small areas where the tissue cannot be observed. To avoid these areas, transparent conductive oxides like Indium Tin Oxide (ITO) can be used. However structures with this material will be not realised because the surface covered by the platinum tracks is sufficiently small so that the largest part of the tissue can be observed to extrapolate the morphology of the slice.

Fabrication process

Glass wafers 500 µm thick and with a diameter of 10 cm were used. Glass has good insulation properties, and thus the electrodes can be directly deposited on this substrate. These electrodes were structured by lift off. First a photoresist layer was patterned by photolithography, then the wafer was covered by a metal layer, and the underlying photoresist was dissolved by using acetone, removing the metal deposited on its surface. The photoresist used for this step

is a positive photoresist S 1400-27 from Shipley. The metal is deposited by evaporation in a vacuum chamber with a source heated by e-gun. A 250 Å thick layer of tantalum was used as adhesion layer prior to the evaporation of 1250 Å of platinum during the same pump-down process. The ratio of the photoresist's thickness to the metal's thickness had to be sufficient in order to enhance the dissolution made with acetone. The main difficulty of this technology is to avoid the formation of wing tips on the perimeter of the electrodes. These are due to the deposition of the metal on the sidewall of the photoresist. A control of the photoresist's profile, related to a sufficient verticality of the deposition, has to be performed to prevent this wing formation. An overhanging profile has to be formed in order to protect the bottom part of the photoresist during the deposition. One of the method commonly used to obtain this result, is to harden the surface of the photoresist before its development by immersing the wafer in chlorobenzene [6]. The method with chlorobenzene is considered to be less efficient with the recent photoresists but an overhang profile can be nevertheless built [7]. A photolithography of high quality, as far as the sidewalls are concerned, is a prerequisite to profit from the advantage of this method. This photolithography is obtained by using a vacuum contact mode during the exposure consisting in realising a close contact between the mask and the wafer, obtained by creating a vacuum in a volume whose limits are the mask and the chuck which support the wafer. The mask is therefore pushed on the wafer by the atmospheric pressure, without an air gap between them.

The top passivation layer consists of a 2500 Å thick PECVD (plasma enhanced chemical vapour deposition) silicon nitride layer. This layer is deposited, at a temperature of 350 °C, in a plasma chamber. Its properties as passivation layer are less efficient than those of the LPCVD (low pressure chemical vapour deposition) silicon nitride. The hydration occurs more rapidly when the device is immersed in a saline solution, and the density of pin holes is higher. But the temperature required for a LPCVD silicon nitride, about 800 °C, is too high for

a normal glass substrate. Quartz would circumvent this limit but the quality of PECVD silicon nitride is considered as sufficient to justify the use of a less expensive material. The silicon nitride layer was etched in a SF_6/O_2 RIE (reactive ion etching) plasma to open the active electrode areas (10 μm in diameter) and the bonding pads defined by a photolithography. A cleaning by using an acidic solution called pirhana was performed in order to etch the photoresist residues after an acetone stripping as well as the redeposition produced by the plasma. The pirhana consists of a mixture of sulfuric acid 96% and a few drops of peroxide 30%. The fabrication process is illustrated in fig. 3.1.

Realised structure

An electrode array is shown in fig. 3.2. and a close up of one electrode is shown in fig. 3.3. The dimensions of the fabricated MEA's are indicated in table 3.1.

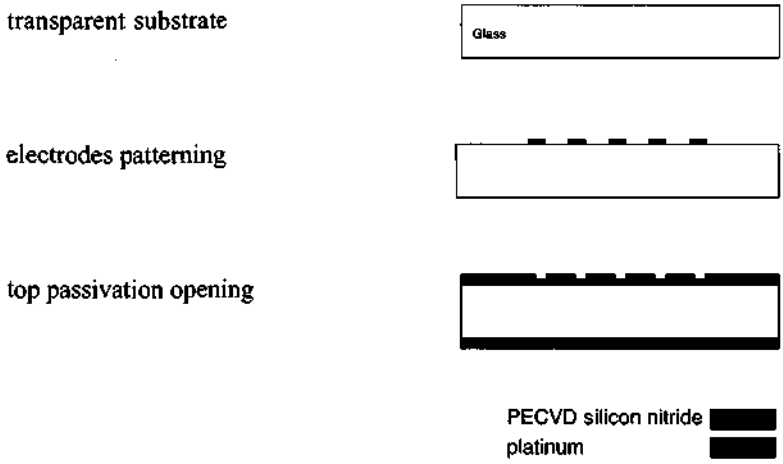

Fig. 3.1. Fabrication process of a MEA on a glass substrate.

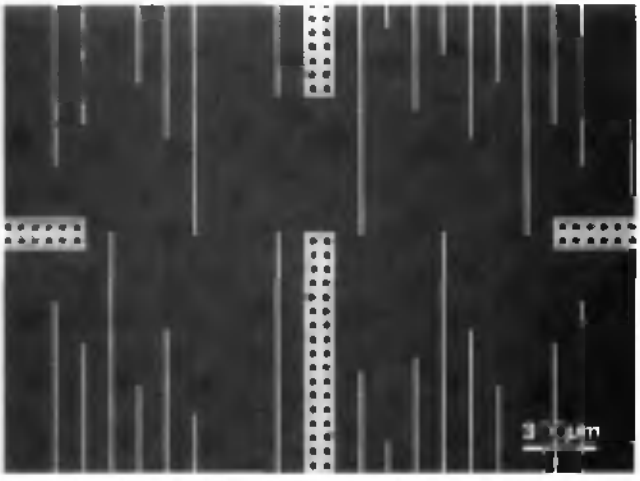

Fig. 3.2. Photograph of a MEA on a glass substrate.

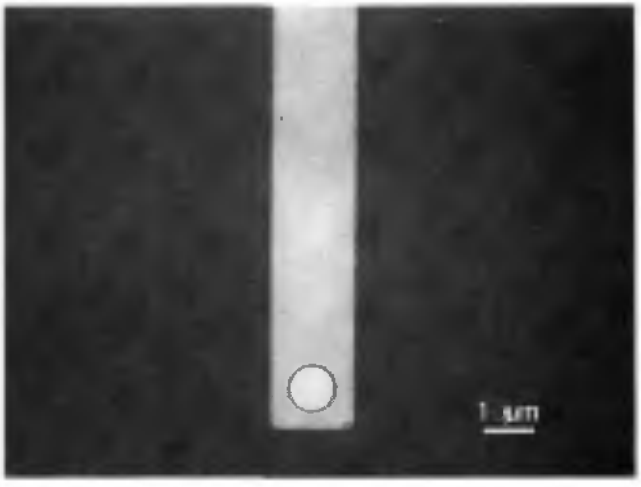

Fig. 3.3. Photograph of one electrode on a glass substrate.

Table 3.1. Dimensions of the planar MEA on glass.

chip dimensions	6 mm x 8 mm x 0.5 mm
microelectrode diameter	10 µm
number of electrodes	30
lateral spacing	120 µm
geometry of the electrodes	double elliptical
big axis of the ellipses	1.8 mm x 1.2 mm / 2.4 mm x 1.8 mm

The electrodes are arranged in an elliptic geometry to match the soma of the pyramidal cells in hippocampal slices from six days old rats, described in paragraph 2.2. Four on-chip reference platinum electrodes, fabricated at the same time as the microelectrodes, are also provided on the substrate.

This chip is fabricated by a relatively simple process: two photolithographies and two layers depositions. As it will be explained in paragraph 4.2., if the electrodes are improved by a surface modification in order to obtain a lower impedance, this device is similar to those available on the market described in paragraph 1.1. Another kind of electrode's modification performed in this study, will be described in paragraph 3.4. The main drawback of these MEAs on this type of glass is the non-porous aspect of the substrate, prohibiting their use for long term organotypic culture by interface.

3.2. Microelectrode array on a perforated membrane

A more complex structure consists of a perforated substrate allowing an access of the nutritive solution and the gas exchanges occurring even on the bottom side to the tissue slice. The substrate usually used for organotypic cultures by interface is the Millicell-CM membrane from Millipore. This porous material

acts as a sponge, absorbing the nutritive solution. A microtechnological method to realised a porous substrate has to be found.

Perforation method

The process used consists of a C_2ClF_5/SF_6 plasma applied on silicon. This process does not allow to obtain holes with acceptable diameter to depth ratio, together with vertical walls, and at an sufficient etch rate. As a consequence, the substrate is made first thinner by anisotropic wet etching on the parts which will support the MEAs.

Fabrication process

The silicon wafer, oriented in the <100> direction of its crystalline structure, is first passivated by a growth of 800 Å silicon oxide and by a deposition of 1800 Å LPCVD silicon nitride. The combination of these two layers shows adequate insulation properties when immersed for a long time in a saline solution like the culture medium [8]. 1500 Å platinum electrodes with an adhesion layer of tantalum were deposited on this substrate and structured by mean of a lift off technique. A photolithography was performed with a 6.5 µm thick AZ 4562 photoresist from Shipley which served as mask for the silicon plasma etching. The silicon nitride was etched by a SF_6/O_2 plasma and the silicon dioxide in buffered HF (BHF) and then only the silicon was etched by a C_2ClF_5/SF_6 plasma with the same photoresist. The time of this silicon etching was determined when the undercutting became too important and was fixed at 50 min, resulting in 15 µm deep holes in the centre of the wafer. All plasma processes, due to the well known border effects, etch at different rates along the radius of the wafer, the lowest etch rate appearing in its centre. This etch rate depends strongly on the diameter of the holes; those with a bigger diameter are etched more rapidly. The use of the C_2ClF_5/SF_6 plasma compared with SF_6/O_2 plasma minimises the effects of undercutting and inhomogeneity in the etch rate of various diameters allowing to fabricate holes with a diameter from 5 µm to 40 µm. The advantage of using a single but thicker photoresist layer

for all the etchings, is that it avoids the misalignments of the successive photolithographies. After the holes etching, a top passivation layer of 2500 Å of LPCVD silicon nitride was deposited on the wafer. This method allowed to coat the whole surface including sidewalls and bottom parts of the holes. The top passivation layer was etched by a SF_6/O_2 RIE plasma after a photolithography in order to open the 10 μm by 10μm electrodes and the contact pads. Just before the spinning of the photoresist, all the holes were carefully filled with photoresist to avoid uncovered areas and air bubbles. This excess of photoresist in the holes induced small changes in the thickness of the layer, easily compensated by sufficient exposure and development. At the same time, a photolithography was performed on the back side of the wafer to define the membrane. On this back side, the insulation layers were etched by SF_6/O_2 plasma for the silicon nitride and BHF for the silicon dioxide. The stripping of the photoresist was made in piranha to remove the redeposition produced by the plasma on the MEA. The formation of the membrane in the silicon was made by wet etching in KOH 40 % at 60 °C. The particularity of this etching consists in an anisotropy due to the differences of the etch rate according to the crystalline plan of the silicon. The plans <100> are etched several hundred times faster than the <111> plans, forming a typical shape of the structure with an angle of 54.7 ° between the wafer's surface and the sidewalls of the membrane. The etching was stopped when the whole bottom parts of the holes, protected by the silicon nitride, were apparent. In this way, the inside part of the holes was not etched by the KOH in spite of the differences of holes depth and the inhomogeneity of the etching. The thickness of the membrane is thus given by the less deep holes, in this case 15 μm. Concerning the inhomogeneity of the KOH etching, the wafer is placed horizontally, the surface to structure above, to prevent the bubbles produced by the chemical reaction, from slowing

the etching by sliding on the silicon. The remaining silicon nitride layer was etched by plasma from the back side in order to finally open the holes. The fabrication process is illustrated in fig. 3.4.

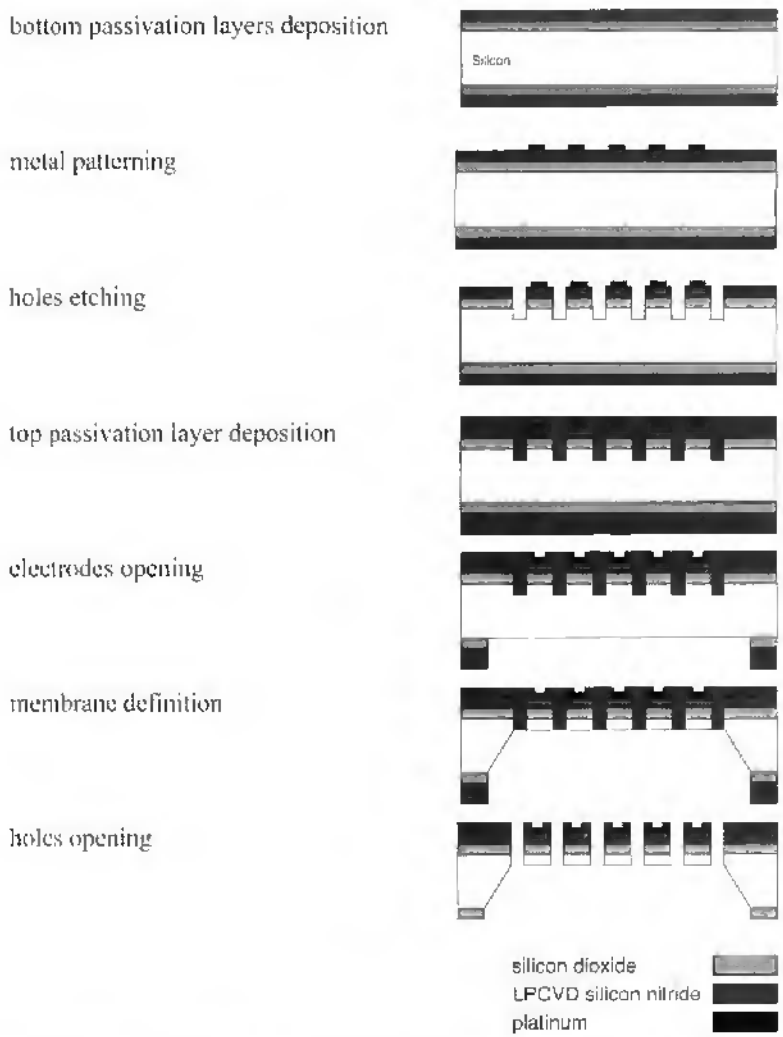

Fig. 3.4. Fabrication process of a MEA on a perforated silicon membrane.

Realised structure

The dimensions of the fabricated MEA's are indicated in table 3.2. Photographs of the top and the bottom side of the membrane of one fabricated chip is shown in fig. 3.5. A transverse view of a perforated structure on a thin silicon membrane is shown in fig. 3.6. This last picture illustrates well the mechanical fragility of the silicon membrane. It can easily be broken, especially during the manipulations of the slice with the tweezers. To circumvent this difficulty, the necessity of a more solid substrate was highlighted. Nevertheless, the tests of cells cultures using these devices established several characteristics which will have to be fulfilled for the next generation of MEAs:

minimum porosity: 20 %
maximum holes diameter: 40 µm

Table 3.2. Dimensions of the planar MEA on a perforated silicon membrane.

chip dimensions	10 mm x 10 mm x 0.4 mm
microelectrode diameter	10 µm x 10 µm
number of electrodes	20
lateral spacing	200 µm
geometry of the electrodes	double elliptical
big axis of the ellipses	2.5 mm x 1.5 mm / 3 mm x 2 mm
porous area	4 mm x 3 mm
holes' sizes	from 5 µm x 5 µm to 40 µm x 40 µm
porosity	from 3 % to 20 %
membrane thickness	15 µm

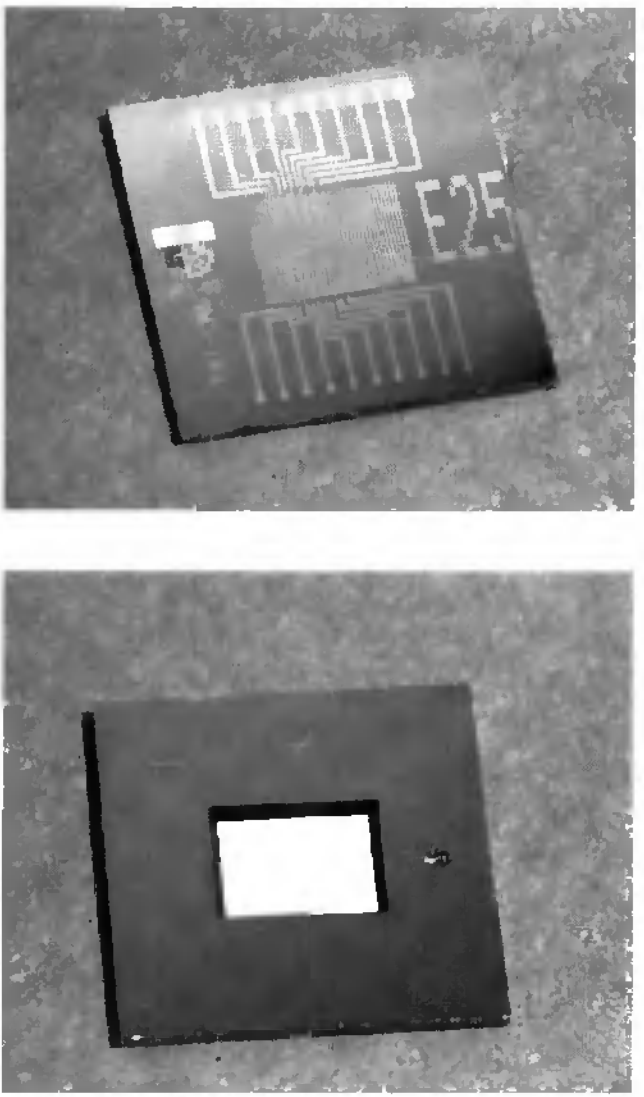

Fig. 3.5. Photographs of the top and the bottom side of a 1 cm by 1 cm chip with a MEA on a perforated silicon membrane.

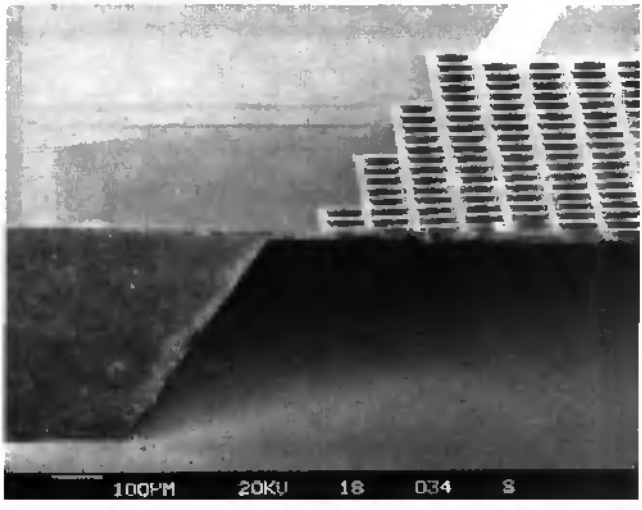

Fig. 3.6. SEM picture of a perforated silicon membrane.

A porosity of 20% is the lowest value to ensure a good viability of the slice on a perforated substrate. The holes diameter has to be 40 µm or smaller to avoid that too much biological material slides into them. From a technical point of view, the diameter of the holes has to be as large as possible in order to increase the ratio of the diameter to depth and thus to enhance their perforation by the plasma. Another advantage of large holes is that the small biological particles, often present inside them after an experiment, can be removed in an easier way. This cleaning is necessary to allow several uses of the MEA. In comparison to a glass substrate, observations of the cultured slices are impossible by a microscope with diascopic illumination. However, due to the good reflectivity of the silicon nitride surface, microscope with top side illumination allows the operator to analyse his experiment.

3.3. Microelectrode array on a perforated aubatrate

A method has to be found to perforate a substrate thicker than a thin silicon membrane. This method should structure the several hundred thousands of via holes with a maximum diameter of 40 µm at the same time on a wafer. This requirement excludes all methods in which holes are perforated one after one like laser drilling or electro discharge machining (EDM). To ensure a sufficient density of holes, the underetching should be low, in order to prevent the neighbouring holes from interconnecting during the etch of a thick substrate. That means that the ratio of the diameter to depth has to be very low, also for a depth of several hundreds µm.

Choice of the perforation method

1) The first option consists in the use of photostructurable glass [9, 10]. This particular glass is structured in three steps. First the glass is exposed to a UV light at a wave length of 312 nm. This process forms silver ions Ag^+ in the exposed area on the whole thickness of the substrate. Secondly, the glass is heated up to about 600 °C. During this thermic treatment, a nucleation occurs around the silver ions to form a ceramic. And finally this ceramic is etched in 10% HF. The etching takes place around the grains of the ceramic, forming a rugosity of 10 µm inside the holes. In this application, the rugosity should not affect the transport of nutritive solution. But the transparency, which represents the main advantage for the use of glass, is lost on the etched surface because of this rugosity. The etch rate of the glass compared with the one of the ceramic is 1/20, forming a hole's profile at an angle of 5° with a vertical axis. This underetching is too important, even if the etching is performed from the back side only. As an example, is a 400 µm thick wafer, which is the minimum to keep a certain mechanical solidity, the hole's diameter is increased by more than 40 µm, resulting in a back side surface nearly totally etched and non-

transparent. Moreover the biocompatibility of this material, which contains a lot of ions, has not yet been established

2) Silicon can be made porous by using an electrochemical process in HF solution under illumination [11, 12, 13]. Holes are formed along the <100> direction with diameters in the range of nm to 20 μm, according to the conditions of the process and the conductivity of the silicon. The length of the pores can be sufficient to go through the whole thickness of the wafer. The porosity can be formed on the whole surface of the silicon or be controlled by a photolithography: the holes are formed from initiation areas which are patterned by a plasma etching or by a wet etching in KOH after a mask transfer.

3) We have selected a plasma based technology: the deep reactive ion etching (DRIE) of silicon. Two approaches exist: the first one consists of a cryogenic cooling of the substrate during the etching, used with the equipment provided by Alcatel and the other, called inductively coupled plasma (ICP), is made by Surface Technology System and is based on the Robert Bosch GmbH patent [14]. The principle consists of a plasma with two alternative steps: the first one is an etching with SF_6 gas, followed by a passivating deposition film using C_4F_8 gas. During this step, a teflon-like material is deposited inside the hole which is preferentially removed at the bottom side during the etching step, forming a sidewall protective layer [15, 16]. The masking materials which can be used for this plasma are photoresist with an etch rate ratio of 1/40 in comparison with that of the silicon, silicon dioxide with an etch rate ratio of 1/200, or also aluminium which has no observable etching rate. This technology gives the opportunity to fabricate a great variety of different structures with a great deepness and vertical sidewalls like the array of holes required for this application [17].

Fabrication process

The beginning of the process is similar to the technology described previously. A 390 μm thick silicon substrate is passivated by 1000 Å of thermally grown

silicon dioxide and 2000 Å of LPCVD silicon nitride. The platinum electrodes with an adhesion layer of tantalum are structured by lift off. The top passivation layer consists of a 2000 Å thick LPCVD silicon nitride, etched by a SF_6/O_2 RIE plasma after a photolithography in order to open the active area and the contact pads. A stripping in an O_2 plasma is applied to remove all the redepositions produced by the plasma. A photolithography using a 10 µm thick AZ 4562 photoresist from Shipley is performed for the etching of via holes. To obtain this thickness, the photoresist is spinned on the Gyrset system from Karl Süss, which consists of a cover plate, rotating at the same speed as the wafer. Under this plate, a layer of an atmosphere saturated in solvent, protecting the photoresist from frictions, allowing a greater resin thickness for a given spin speed to be deposited. Then the silicon nitride is etched by a SF_6/O_2 RIE plasma and the silicon dioxide in BHF. The perforation of the holes (35-40 µm in diameter) is made by DRIE with the same photoresist through the whole thickness of the wafer during typically 150 min.

The etching, first of the passivation layers and then of the holes can also be made with two photolithographies. In this case, thinner photoresists are spinned, respectively 2 µm of AZ 1518 during the etching of the passivation layers and 7.5 µm of AZ 4562 during the etching of the silicon, both provided by Shipley. These photolithographies require no Gyrset option and allow a more precise alignment with the electrodes but induce a small shift between the passivation layers and the silicon holes. The consequence of this shift is the formation of an underetching at the top parts of the holes.

The etch rate differs according to different parameters. First, the borders are etched more rapidly because of the border effect of the plasma. The size of the structures also plays a great role: small patterns are etched more slowly than bigger ones. For that reason, all the holes in this design have the same diameter. One explanation for these differences according to the size might be the evacuation of the elements resulting from the chemical reactions which occur

during the etching. The diffusion of these compounds is hindered in the bottom part of the narrow holes with the result that the etch gas is diluted in this area. This phenomena can also explain the parabolic-like shape of the front of the etching. Actually, the centre of these small holes is etched more rapidly than the borders. Another explanation of the different etch rates according to the size of the structure, is the non-verticality of the etch ions incidence. Some of them react with the sidewall before reaching the silicon. With all these effects, the holes are first etched in the perimeter of the wafer and with a small aperture. The back side silicon dioxide layer, deposited during the first step of this process, acts as etch stop and enhances the etching of the sidewall. An overetching is thus performed to enlarge these backside apertures. The protecting layer of the sidewalls prevents efficiently the etching by the non-vertical ions as well as the reflected ones. So, no observable underetching occurs and the diameters are identical to the mask design except in the middle part of the deep holes. This can be explained by the fact that when the etch rate of the bottom area begins to be significantly reduced, the diameter of the holes is enlarged by the phenomena mentioned above, in order to enhance the etching by allowing more gas exchanges. From a certain deepness the etching conditions are changed and some tips structures appear on the sidewalls, similar to these formed on black silicon [18]. These poor quality sidewalls are formed from a depth of about 200 μm. The fig. 3.7. and 3.8. show the resulting perforated holes and illustrate the effects described above.

The end of the process consists of the etching of the back side passivation layers which still obstruct the holes by a SF_6/O_2 RIE plasma for the silicon nitride and by a BHF dip for the silicon dioxide. This BHF etching also removes, by underetching, a thin part of the silicon dioxide deposited on the front side, between the silicon nitride and the silicon. This is shown in fig 3.9. with the upper part of the holes. This underetching can be avoided, if necessary, by a

photoresist deposition on the top side obtained by the use of an aerograph for instance. The fabrication process is illustrated in fig. 3.10.

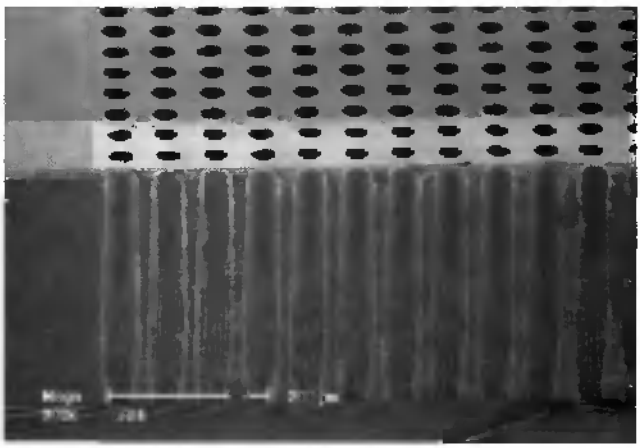

Fig. 3.7. SEM picture of a 390 µm thick silicon chip perforated by DRIE.

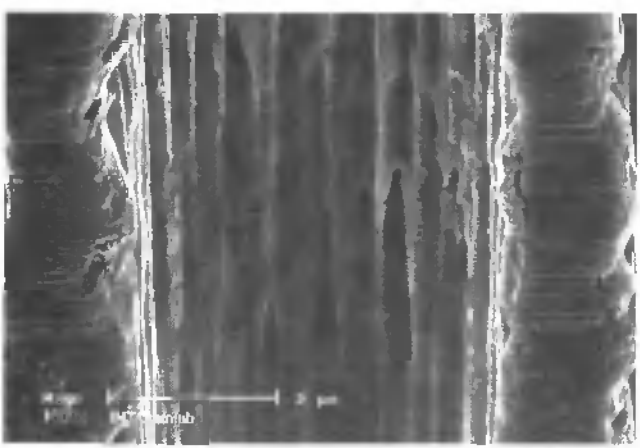

Fig. 3.8. SEM picture of a close up view of the bottom part of the holes.

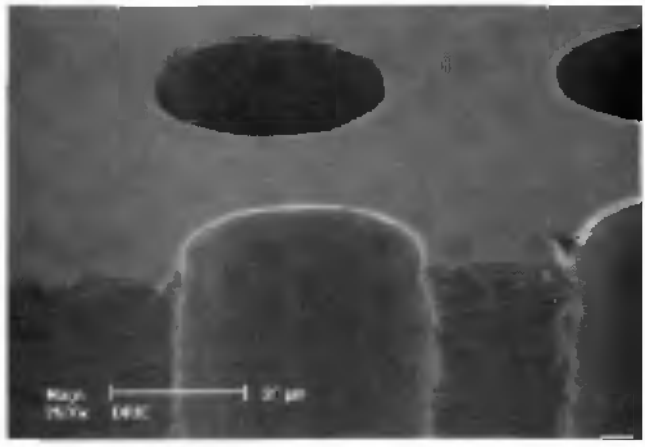

Fig. 3.9. SEM picture of a close-up view of the upper part of the holes.

bottom passivation layers deposition

metal patterning

top passivation layer deposition

photolithography

DRIE holes etching

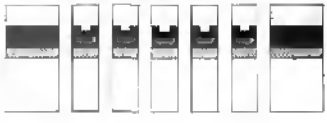

Fig. 3.10. Fabrication process of a MEA on a perforated silicon substrate.

Realised structure

The dimensions of the fabricated MEA's are indicated in table 3.3. This substrate allows a good viability of the slices cultures as it will be shown in paragraph 4.4. and its mechanical robustness is adequate for all manipulations. The tips structures inside the bottom parts of the holes do not affect the liquid transport during the culture.

Table 3.3. Dimensions of the two designs of planar MEA on a perforated silicon substrate.

chip dimensions	10 mm x 10 mm x 0.4 mm or 8 mm x 6 mm x 0.4 mm
microelectrode size	10 µm x 10 µm or 10 µm in diameter
number of electrodes	20 or 30
lateral spacing	200 µm or 120 µm
geometry of the electrodes	double elliptical
big axis of the ellipses	2.5 mm x 1.5 mm / 3 mm x 2 mm or 1.8 mm x 1.2 mm / 2.4 mm x 1.8 mm
porous area	4 mm x 3 mm
holes' sizes	40 µm x 40 µm or 35 µm in diameter
porosity	20 % or 25 %

In summary, the DRIE technology allows a suitable devices for the organotypic culture by interface to be achieved. In the next step, the electrical characteristics of the planar MEAs will be improved.

3.4. Three dimanaional microelectrode array

The structures presented above are made up of planar microelectrodes. This paragraph will describe a post-process step which can be applied to all these structures in order to give a three dimensional aspect of their electrodes. This process is a electrochemically based growth to form platinum hillocks starting from the planar electrodes. This electroplating principle consists in the reduction of a dissolved platinum compound (hexahydroxy platinic acid) on the microelectrodes, at a voltage of about -0.7 V versus a reference electrode. The metal deposition is achieved by cyclic voltammetery, which is more reproducible and results in geometrically better defined three dimensional electrodes in comparison with the more classical galvanostatic electroplating. Due to the satisfactory achievements realised with platinum, no tests were performed on other biocompatible metal which can also be electroplated, like gold for example [19].

Preparation of the substrates

The platinum growth takes place on all the connected conductive material, thus the chip is mounted on a printed circuit board (PCB), the same which will be later used for the electrophysiological experiments. The electrical contacts between the chip and the PCB are made by bonding and are encapsulated manually with epoxy. Then the microelectrodes are pre-treated by cyclic voltammetry in a 1M H_2SO_4 solution. The equipment used consists of a three electrodes set-up controlled by an IBM Voltammetric Analyser (EC/225). The MEA acts as working electrode and the voltage is scanned from -0.3 V to 1.6 V versus the reference electrode, a saturated calomel electrode (SCE), at 100

mV/s. The counter electrode is a platinum wire. The voltammogram allows first to verify the platinum quality as shown in paragraph 4.3. and then to perform a cleaning and a small modification of the surface making it slightly rougher [20]. A clean surface together with this morphology change, allows a better anchorage for the following platinum deposition to be achieve.

Platinum growth

The platinum deposition is performed by cyclic voltammetry in a commercially available solution: platinum solution 3745 from Engelhard, containing hexahydroxy platinic acid. The set-up is identical to that used for the pre-treatment. The potential range goes from 0 V to -0.75 V versus SCE at a scan rate of 50 mV/s. The typical measured voltammograms are shown in fig. 3.11.

Fig. 3.11. Voltammograms of the platinum deposition.

On these curves, the reduction peak is clearly visible. The amount of the deposited platinum is related to the sum of the integral of each cycle but the current at the reduction peak can serve as an indicator. As expected, the growth of platinum layer is accompanied by an overall enlargement of the structure. The expansion of the contact surface with the electrolyte can be observe on the voltammograms by the increase of the current peak. The deposition takes place according to the density of the electrical field and begins mainly on the border of the flat electrodes before forming a hemispherical shape, like illustrated on fig 3.12. The deposited material has an important internal stress, producing the cracks which can be observed on the SEM photographs. The mechanically weakest part is the base of the structure, notably on account of this stress. For this reason, at the beginning of the process, the temperature of the deposition is at room temperature, and is then increased up to 50 °C in a thermostatic bath. By that mean, the growth rate is slower in the beginning of the deposition, improving the mechanical stability of the hillock by reducing the internal stress. The temperature of the deposition has then to be increase to obtain a sufficient growth rate.

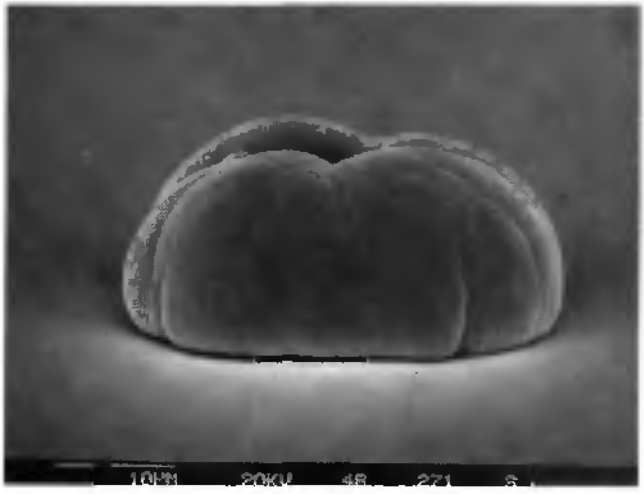

Fig. 3.12. SEM picture of the platinum hillocks.

Another aspect consists in the fact that the deposition has to be made in one step. If the process is interrupted, the microelectrode rinsed in water and the process then continued, a clear interface appears between these two phases as illustrated on fig 3.13.

The deposition is stopped when the height of the platinum reaches 20 µm. A thickness up to 35 µm were obtained, but a height of 20 µm happened to be the best compromise between the desire to obtain the maximum electrode height on the one hand and the broadening of the electrodes during the platinum electroplating and the mechanical stability of the hillock on the other hand. This height corresponds to a current peak of 85 µA for 20 electrodes or a deposition time of 45 minutes. The criterion of the current value is valid only if no parasite platinum depositions are built. There are two main causes of these unwanted formations. First, the pinholes of the top insulation layer, if they are located on the metal tracks. Secondly, the wings tips remaining sometime after the lift off, which are then recovered by the top insulation layer, can be broken later on in

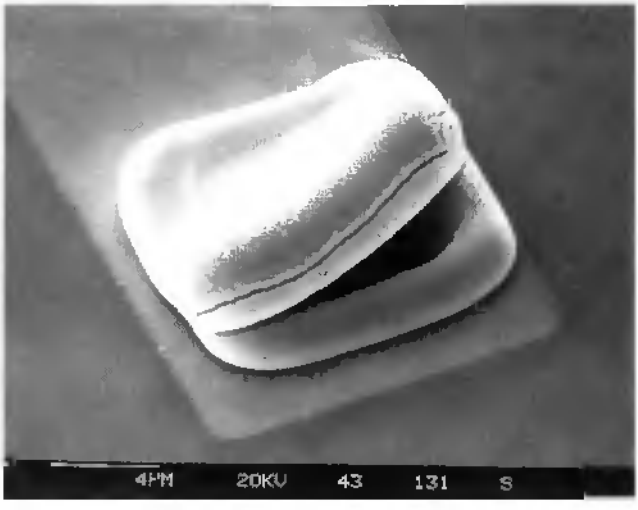

Fig. 3.13. SEM picture of the platinum hillocks deposited in two steps.

the process, creating an apparent thin metallic line. These parasite formations can be easily seen with a microscope, and thus their impact on the measurements can be evaluated. If the surface of hillocks is observed by using a SEM, the platinum shows a smooth appearance forming a bright aspect as illustrated on fig 3.14.

Compared with the black platinum, there is no formation of thin and fragile shapes and this fact allows several manipulations of the devices without the risk of damaging their surface. The number of utilisation is however limited because of the mechanical fragility of the base of the structure. A verification by the microscope after each utilisation permits to know if some electrodes are broken.

Realised structure

A device with electroplated hillocks is shown in fig. 3.15. The dimensions of the fabricated electrodes are indicated in table 3.4.

Fig. 3.14. SEM picture of the platinum hillocks surface.

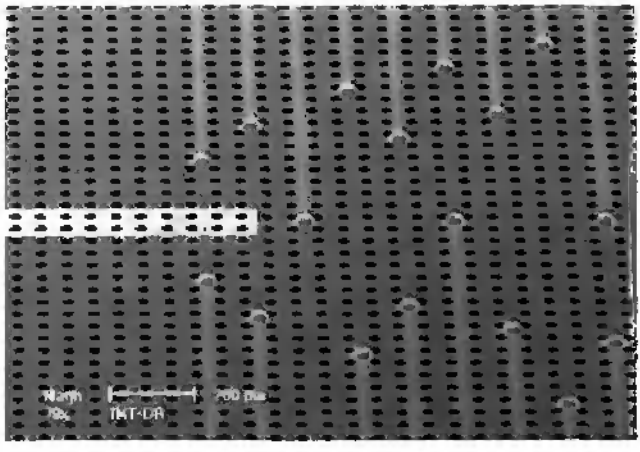

Fig. 3.15. SEM picture of a MEA with platinum hillock shaped electrodes.

This device has a perforated area required for organotypic culture by interface and three dimensional platinum electrodes to enhance the measurements. With a height of 20 µm, these electrodes have a closer contact with the slice and reduce the distance between them and the soma of the neurons layer. The surface of the hillocks is considerably larger than of the planar electrodes and allows a good electrical coupling with the extracellular medium. This fact will be highlighted in the chapter 4 and in [21] by the very low value of the impedance and the high amplitude of the voltage recording during the electrophysiological measurements. The main limitation for the use of this device consists in the mechanical fragility of the three dimensional structures. This fragility limits the manipulation of the slice which has to be moved very carefully and reduces the number of use.

Table 3.4. Dimensions of the platinum hillock shaped electrodes.

microelectrode size	40 µm x 40 µm x 20 µm

3.5. Platinum tip microalectrode array on a perforated aubatrate

In this process, the three dimensional electrodes will be formed in the bulk of silicon in order to enhance their mechanical stability. The technology necessary to achieve this result consists in silicon tips, shaped by underetching. A silicon anisotropic wet etching was performed under a mask deposited on the surface of the wafer, up to the etch planes met each other to form a tip, as first presented in [22] and adapted at our institute [23]. After this tips formation, passivated electrodes can be embedded. In this way, an array of platinum tips with a height of about 50 μm, open only on the top, will be realised. This size, as well as this shape, allow the electrodes to penetrate into the cultured tissue in order to reach the layer of the neurons' soma.

Fabrication process

The devices were fabricated on a 390 μm thick <100> silicon wafer. In the first step, 3600 Å of silicon dioxide, the etch mask for the tips, was grown by thermal oxidation and then patterned in a BHF solution after a photolithography. The design of this etch mask, determined by preliminary tests, consisted in an octagon of 190 μm in diameter. The silicon tips were formed by anisotropic etching with KOH 40% at 60 °C. The etching of 55 μm of silicon resulted in 47 μm high tips as shown in fig. 3.16. A slightly rough surface is formed on the (100) plane of the wafer with this etching. These irregularities did not affect neither the cultures nor the following technological steps.

1000 Å of silicon dioxide and 2000 Å of silicon nitride layers were deposited by thermal oxidation and LPCVD respectively to make the bottom passivation. The metallic layers were patterned by using a lift off process. Here, a negative photoresist (ma-N 420, Micro Resist Technology), soluble in acetone, was used to achieve overhanging profiles favourable for the lift off [24]. Actually, by

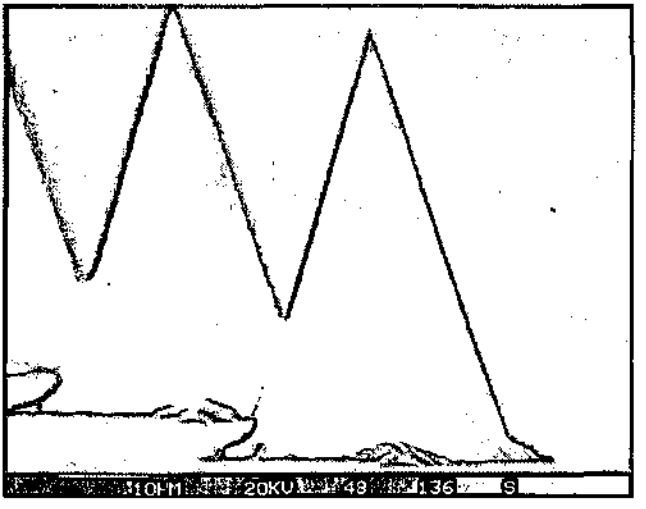

Fig. 3.16. SEM picture of 47 μm high silicon tips.

overdeveloping it, negative slopes were formed, although no vacuum contact mode exposure was applied. In this case, a close contact between the mask and the wafer could not be performed because of the tips. To protect them, the mask was blocked by stoppers formed by the original surface of the wafer remaining after the tips formation, 55 μm higher. After the photolithography, a short O_2 plasma at room temperature was performed to remove the remaining photoresist traces often present with ma-N 420. A 200 Å thick adhesion layer of tantalum and a 1300 Å thick layer of platinum were evaporated showing an adequate covering of the slopes of the tips as illustrated in fig. 3.17.

The top passivation consisting of 2000 Å of LPCVD silicon nitride was deposited and patterned by a SF_6/O_2 RIE plasma, by using a thick photoresist photolithography technology developed at our institute [25]. A photoresist layer of about 42 μm high had to be spinned with the Gyrset system to protect the bottom side of the tips. The photoresist was removed by the photolithography on the contact pads and on the upper part of the tips at the same time. An

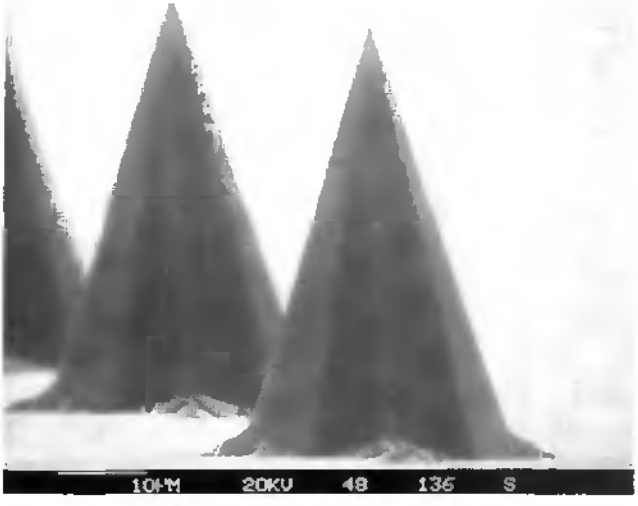

Fig. 3.16. SEM picture of 47 µm high silicon tips.

overdeveloping it, negative slopes were formed, although no vacuum contact mode exposure was applied. In this case, a close contact between the mask and the wafer could not be performed because of the tips. To protect them, the mask was blocked by stoppers formed by the original surface of the wafer remaining after the tips formation, 55 µm higher. After the photolithography, a short O_2 plasma at room temperature was performed to remove the remaining photoresist traces often present with ma-N 420. A 200 Å thick adhesion layer of tantalum and a 1300 Å thick layer of platinum were evaporated showing an adequate covering of the slopes of the tips as illustrated in fig. 3.17.

The top passivation consisting of 2000 Å of LPCVD silicon nitride was deposited and patterned by a SF_6/O_2 RIE plasma, by using a thick photoresist photolithography technology developed at our institute [25]. A photoresist layer of about 42 µm high had to be spinned with the Gyrset system to protect the bottom side of the tips. The photoresist was removed by the photolithography on the contact pads and on the upper part of the tips at the same time. An

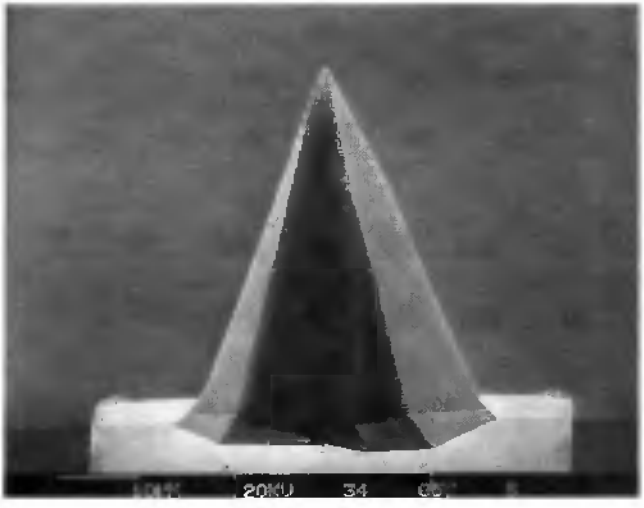

Fig. 3.17. SEM picture of a tip after platinum deposition.

alternative method of photoresist deposition to open the upper part of a tip, consists of adapting the photoresist's thickness, in order to match the area where the passivation has to be removed. This limit is given by the rising of the photoresist on the slope of the tips during the spinning, until the film becomes too thin to go higher. This method has the drawback to open different surface area due to the differences of the photoresist layer thickness on the wafer. An opening by photolithography is then preferred in our case to obtain a more reproducible active area of the electrodes on the whole wafer. Nevertheless this method by sliding was used for the structures described in paragraph 3.6.3. The difficulty for the alignment is important because of the distance between the mask and the wafer surface. The edge bead which is formed by the photoresist at the border of the wafer during the spinning is removed by acetone to reduce this distance. The resulting misalignment can be observed between the centre of the open area and the top of the tip as illustrated in fig. 3.18. Because of this misalignment, this method cannot be applied to a smaller

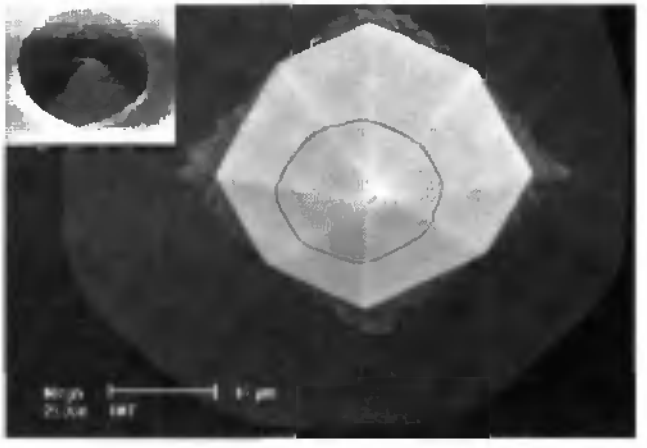

Fig. 3.18. SEM picture of the active area of a tip viewed from the top and the SEM picture of the photolithography performed to achieve the opening of the passivation layer (insert, scale bar 4 µm).

opening. The resulting platinum forms nearly a cone with a base of 10 to 15 µm and a height of 15 to 20 µm. The etching time by the RIE of the silicon nitride deposited uniformly on the tip, was influenced by the inclination of this layer. This plasma etches approximately according to a vertical axis. Compared with it, the angle formed by the slope of the tip is about 20°. The projection of a layer thickness on this axis shows an increase by a factor 3. As a consequence, the etching time of the silicon nitride was increased by the same factor. On the contact pads this layer was flat and a consequent overetching was observed but this etching was stopped by the platinum layer. The next step consisted in the hole arrays perforation by DRIE. A thick photolithography was again required to protect the silicon nitride on the sidewall of the tips. The photoresist layer could not be used directly for this etching because, with the thickness of about 40 µm, it would not withstand the plasma conditions. A postbake could enhance the resistance of the photoresist but a heating would melt it and the design of the hole array will be destroyed. A mask of aluminium 3000 Å thick

was thus preferred but its known high toxicity for the neurons has to be considered. Hence, to be sure that no aluminium traces would remain on the surface, a 4500 Å thick CVD silicon dioxide layer was deposited in-between. After the thick photolithography was performed, the etching sequence in order to reach the silicon was as follows: $SiCl_4/N_2/Cl_2$ plasma to remove the aluminium, BHF for the CVD silicon dioxide, SF_6/O_2 plasma for the LPCVD silicon nitride, and BHF for the thermal silicon dioxide. The aluminium was etched by a plasma instead of using a wet process because of the low wettability of the holes in the photoresist. This effect resulted in the overetching of the aluminium for some holes and in the non-etching for some others. This issue was not so important during the silicon dioxide etching because the BHF solution is more fluid. The alternation of wet and dry etching steps allows to compensate the inhomogeneity of the plasma processes and to have a better defined surfaces. The photoresist was then dissolved in acetone and the 335 µm of silicon could be etched by the DRIE. The resulting holes are similar to those described in paragraph 3.3. with a diameter of 40 µm. The final steps consisted in the removal of several layers: the silicon nitride on the back side by plasma etching, the aluminium by wet etching and finally the CVD silicon dioxide on the top side, at the same time as the thermal oxide on the back side, by using BHF. By that mean the holes were completely open and the MEA usable. The fabrication process is illustrated in fig. 3.19.

oxide mask for tips

anisotropic etching to form tips

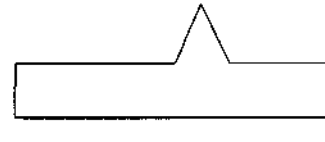

bottom passivation layers deposition

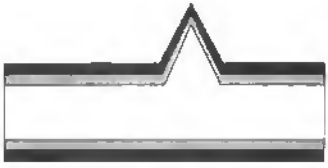

metal patterning

top passivation layer deposition and
thick photolithography

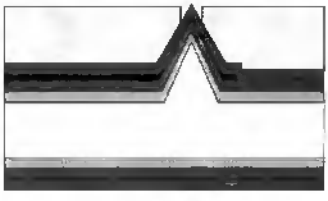

top passivation layer etching

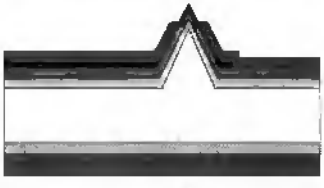

aluminium mask for holes and
thick photolithography

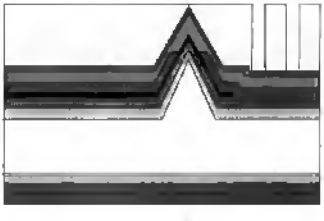

DRIE holes etching

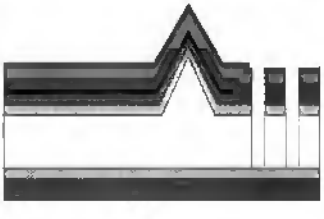

Fig. 3.19. Fabrication process of a platinum tip MEA on a silicon perforated substrate.

Realised structure

The dimensions of the fabricated MEA's are indicated in table 3.5.

Table 3.5. Dimensions of tip shaped MEA on a perforated silicon substrate.

chip dimensions	8 mm x 6 mm x 0.4 mm or 8 mm x 6 mm x 0.3 mm
tip height	47 µm
microelectrode size	cone with a circular base of 10-15 µm in diameter and 15-20 µm high
number of electrodes	34 or 32
geometry of the electrodes	double elliptical or rectangular
1) big axis of the ellipses	1.8 mm x 1.2 mm / 2.4 mm x 1.8 mm
lateral spacing	120 µm
2) rectangular array	2.4 mm x 0.7 mm
spacing	300 µm x 180 µm
porous area	4 mm x 3 mm
holes' sizes	40 µm in diameter
porosity	35 %

The resulting structures with the two designs are shown in fig. 3.20 and a close up of one electrode in 3.21.

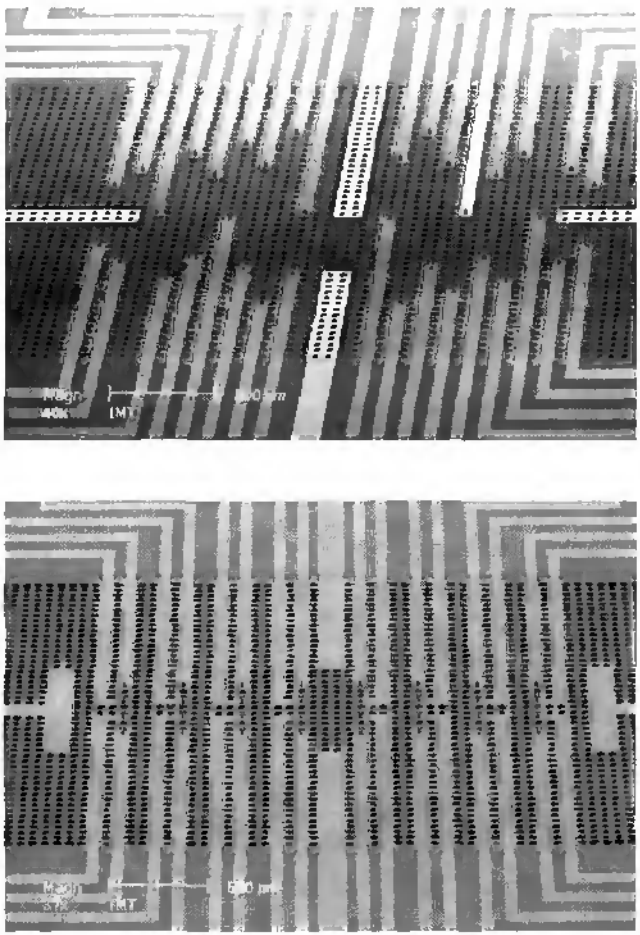

Fig. 3.20. SEM picture of a tip shaped MEA with double elliptical (above) or rectangular (bottom) geometry on a perforated silicon substrate.

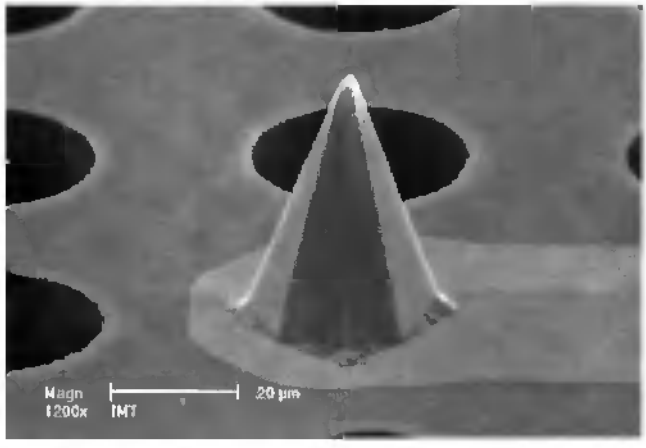

Fig. 3.21. SEM picture of a platinum tip electrode on a perforated silicon substrate.

The two main requirements, determined in paragraph 1.2, in order to monitor the electrical activity of an organotypic culture by interface are fulfilled with this device. The first one consists of a mechanically solid perforated substrate with a porosity of 35%. And the second one is a MEA with a height in the order of 50 µm which can penetrate into the glial cells layer. The tip shaped electrodes realised with a top curvature of 0.5 µm are suitable for that purpose without causing damages on the cells. The 15 µm upper part is exposed platinum as illustrated in fig 3.22. Then tip shaped electrodes can measure the neurons activity, in a more local way than the hillocks. Nevertheless, the surface area of the platinum is smaller in comparison with the hillocks and this resulted in a higher impedance. The characteristics of this electrode will be described in chapter 4, and in [26].

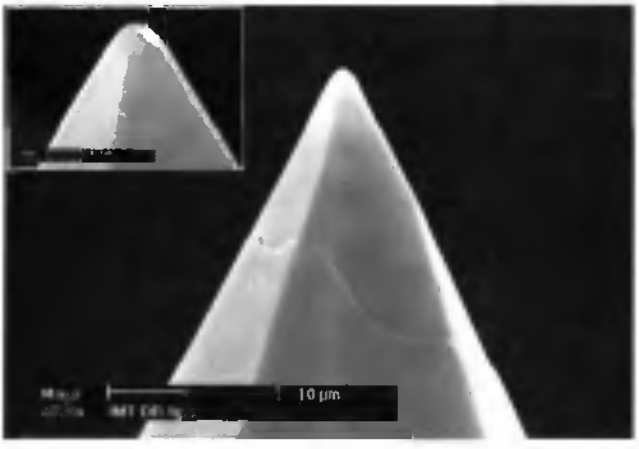

Fig. 3.22. SEM picture of an upper part of a platinum tip electrode and a close up of the tip (insert, scale bar 1 µm).

3.6. Other realisations

During the development of the MEA described in the previous paragraphs, several other devices were fabricated either to test different electrodes geometry or to measure some additional aspects of the neurons activity than the electrical signals. These attempts were not selected as a priority for physiological experiments because of certain drawbacks of these tools or because of changes of interest. These realisations are nevertheless presented as example of some technical possibilities and as intermediate results for further research.

3.6.1. Cylindrical shape microelectrode array

These electrodes are fabricated using an alternative deposition method to the electroplated platinum hillocks presented in paragraph 3.4. In this case, a mould was added on the surface of the chip to straighten the shape of the deposited

platinum. Compared with the half-spherical aspect of the hillock, a thinner and higher form could be obtained. Thus, the relatively unlocalised characteristic and the distance to the neurons of the electrodes can be improved. The mould material consisted of AZ 4562 photoresist, structured by a thick photolithography of about 40 µm high, to obtain mould opening placed above the microelectrodes. This photoresist was deposited on a non porous wafer to avoid that it flows inside the holes. The wafer was diced with this layer and the chip encapsulated before the electroplating was performed as described in paragraph 3.4. The only differences during the platinum deposition process were the following. First, the increase of the current at the reduction peak was not so significant, because the enlargement did not take place. Secondly, the time of deposition was longer because a greater thickness of platinum has to be deposited and, moreover, the growth rate was limited by the diffusion of the platinum ions in the holes. A fabricated cylindrical platinum electrode is shown in fig. 3.23. Unfortunately, this process presents a low reproducibility and the photoresist was often etched in the solution used for the platinum growth which is a strong base. The explanation of this was not carefully investigated

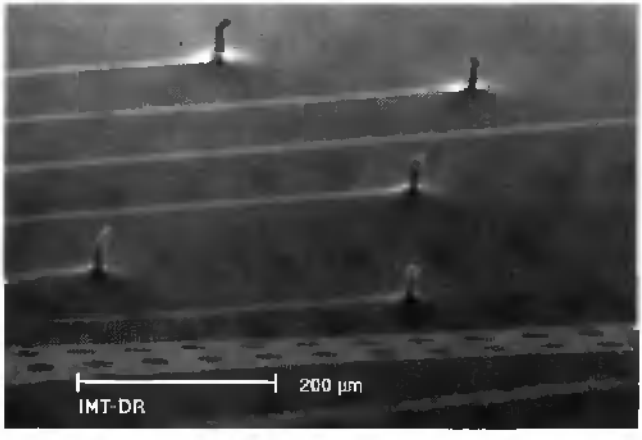

Fig. 3.23. SEM picture of cylindrical platinum electrodes.

but unstability with the time of the characteristics of this photoresist has already been observed, especially when exposed to different humidity levels. For that reason, another mould material was investigated. It consists of an epoxy based negative photoresist called Epon SU-8 provided by Microlithography Chemical Corp. [27, 28]. Very thick structures can be patterned and their resistance to chemical etching is excellent. However, if the electroplating could be performed, the stripping of the mould was difficult. With the materials which constitute the MEA device, even strong etching solutions can be used, like sulfuric or nitric acids. The Epon stripping is in fact not really a dissolution process but small particles are first detached, helped by the high internal stress of this photoresist. By that mean, the mould can be removed but unfortunately the platinum columns are, at the same time, taken away. This experience highlights the main problem of this three dimensional electroplated electrodes which consists in their limited adhesion on the underlying surface.

3.6.2. Platinum tip microelectrode array with a small open area

The tip shaped microelectrodes presented in paragraph 3.5. have an exposed platinum area forming a cone approximately 15-20 μm high and 10-15 μm at the base. If this surface is reduced to an open area of some μm, a more precise location of the electrode will be achieved. This structure can be obtained with one modification in the fabrication process of the tip MEA. First the tips have to be formed in the silicon, and this substrate has to be passivated, then the platinum has to be patterned and the top passivation has to be deposited. At this stage, a thick photoresist was spinned, but only the contact pads were exposed and developed. The top of the tips were left just outside of the photoresist layer. Actually, a few micrometers of the tips remains higher than the thickness of the photoresist layer, according to the method described in paragraph 3.5. and in [29]. The passivation layer was etched with a SF_6/O_2 plasma and the resulting

structure is shown in fig. 3.24. The last step consisted in the holes' perforation using DRIE with a photolithographically defined aluminium mask. The open platinum surface is different along the radius of the wafer according to the differences of thickness of the photoresist. Some structures on the wafer's border are not opened and, in the centre of the wafer, the electrodes have a size in the range of 2 µm in height. To obtain small openings with a better reproducibility, another plasma technology can be applied without photoresist deposition. Based on the accumulation of charge on all sharp structures, a plasma etching of the insulation layer can be performed selectively on all the summits of the tips [30]. Another method uses high voltage discharge to remove the silicon nitride [31]. Nevertheless, if a precise point of measurement is attractive for an electrophysiological experiment, the main drawback of this device is the high impedance value of the electrodes. Hence, the electrical signal is strongly reduced and the tips with a bigger active area are preferred. The comparison between all electrode types is described in paragraph 4.1.

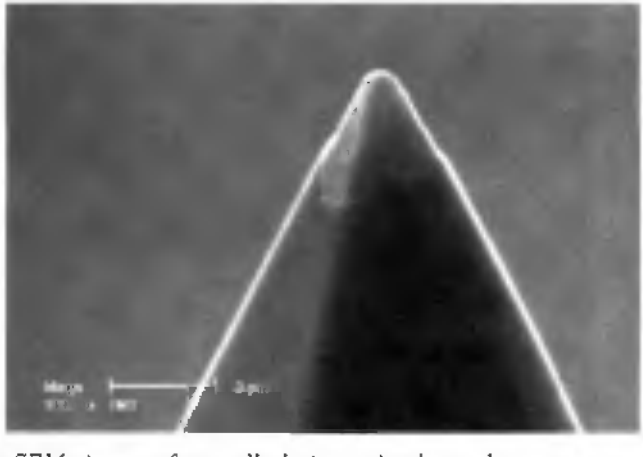

Fig. 3.24. SEM picture of a small platinum tip electrode.

mini-microtips

The tips shaped electrodes presented so far, were adapted for thick slices, such as organotypic cultures. For some other applications, in which the cultured cells form a thin layer, mini three dimensional electrodes can also be considered as an advantage. In this case, mini tips about 3 µm high with an open platinum part about 1 µm high were fabricated on a non-perforated substrate. The technology process involved was similar to that described in the first part of this paragraph, except for some small differences. The first one was of course the realisation of the silicon tips for which a smaller etch mask was used: an octagon of 20 µm in diameter and a shorter etching of the silicon in KOH: a depth of about 6.5 µm. The other adaptation required, concerned the parameters of the photolithography for the opening of the top passivation LPCVD silicon nitride on a such a small tip size. A photoresist S 1813 from Shipley was spinned at a speed of 5000 rpm during 40 s to form the protecting layer of the bottom part of the tip as shown in fig. 3.25.

Fig. 3.25. SEM picture of the photolithography performed to achieve the opening of the passivation layer of a mini-microtips.

After 1 min of O_2 plasma to remove the remaining traces of photoresist, the top passivation was etched with a SF_6/O_2 RIE plasma. Some silicon nitride irregularities were formed near the platinum tip resulting in a less defined metal surface. This mini-microtip is shown in fig. 3.26. Because of a faster spin speed, the reproducibility of the photoresist thickness on the wafer, and thus of the surface of the electrodes, are enhanced in comparison with the thick photolithography.

3.6.3. Carbon interdigitated microelectrode array for dopamine detection

The use of thin film carbon electrodes, arranged in an interdigitated array (IDA), for the electrochemical detection of dopamine was well established [32], also at our institute [7]. In order to add this functionality to the device, such a sensor was integrated on the MEA. A 500 Å thick layer of titanium was deposited after the platinum electrodes patterning on the passivated substrate. In order to structure it, this film was etched by BHF after a photolithography.

Fig. 3.26. SEM picture of a platinum mini-microtip electrode.

Since the electrical resistance of carbon is high, this underlying metal, disposed under the main tracks of the IDA, will reduce the ohmic loss of the measured signal. The carbon, 4000 Å thick, is then deposited by a sputtering process, performed at the CSEM (Swiss Centre for Electronic and Microtechnology). The adhesion of the carbon on the platinum was not sufficient and small particles were detached from the surface and had thus to be removed mechanically in order to continue the fabrication. The realisation of the IDA before the platinum deposition should solve this problem. A 1000 Å thick PECVD silicon nitride layer was deposited to serve as mask for the carbon etching. This mask was structured by a SF_6/O_2 RIE plasma after a photolithography, followed by an O_2 plasma to etch the carbon. The silicon nitride was removed using a BHF solution. The top passivation layer consisted of a 2500 Å PECVD silicon nitride. The presence of carbon did not allow a deposition process at a high temperature like that needed for the LPCVD silicon nitride. The opening of the IDA through the PECVD silicon nitride was performed with BHF to avoid a contamination of the carbon with the plasma. The platinum electrodes and the holes were fabricated like described in paragraph 3.3. The size of the active surface of the IDA was 210 µm by 250 µm. The carbon electrodes were 2 µm wide, and spaced by 2 µm. This sensor, shown in fig. 3.27., remains under evaluation.

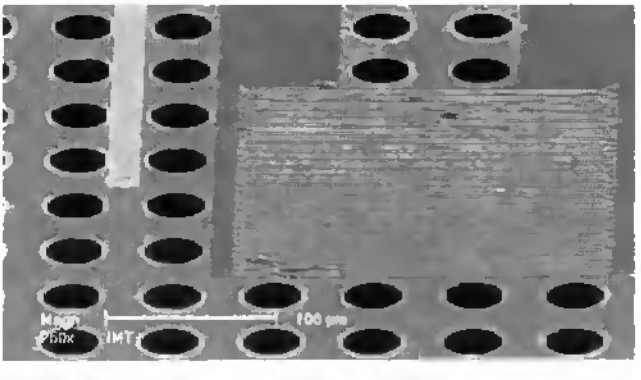

Fig. 3.27. SEM picture of a carbon IDA on a MEA.

References

1 M. Madou "Fundamentals of microfabrication", CRC Press, Boca Raton (USA), 1997

2 S. M. Sze "Semiconductor devices: physics and technology", John Wiley & Sons, New York (USA), 1985

3 W. M. Moreau "Semiconductor lithography: principles, practices, and materials", Plenum press, New York (USA), 1988

4 S. M. Rossnagel, J. J. Cuomo, and W. D. Westwood "Handbook of plasma processing technology", Noyes publications, Park Ridge (USA), 1990

5 P. Rai-Choudhury "Handbook of microlithography, micromachining, and microfabrication", SPIE optical engineering press, Bellingham (USA), 1997

6 M. Hatzakis, B. J. Canavello, and J. M. Shaw "Single-step optical lift off process", IBM J. Res. Develop., vol 24, 1980, p. 452-460

7 G. C. Fiaccabrino "Thin-film microelectrode arrays: materials and designs", Thesis dissertation, University of Neuchâtel, 1996

8 D. J. Edell, "A peripheral nerve information transducer for amputees: long-term multichannel recordings from rabbit peripheral nerves" IEEE transactions on biomedical engineering, vol. 33, 1986, p.203-214

9 "FOTURAN-a material for microtechnology" Schott/IMM information, Mainz (Germany)

10 T. Dietrich "Photostructuring of glass" course organized by FSRM, Neuchâtel (Switzerland)

11 R. L. Smith and S. D. Collins "Porous silicon formation mechanisms", J. Appl. Phys., vol 71, 1992, p. R1-R22

12 V. Lehmann "Porous silicon-a new material for MEMS", Proceedings of IEEE Micro Electro Mechanical Systems, San Diego (USA), 1996, p.1-6

13 H. Ohji, P. T. J. Gennissen, P. J. French, and K. Tsutsumi "Fabrication of accelerometer using single-step electrochemical etching for microstructures (SEEMS)", Proceedings of IEEE Micro Electro Mechanical Systems, Orlando (USA), 1999, p.61-65

14 F. Laermer and A. Schilp of Robert Bosch GmbH "Method of anisotropically etching of silicon", US Patent n° 5501893

15 A. A. Ayon, R. A. Braff, C. C. Lin, H. H. Sawin and M. A. Schmidt "Characterization of a time multiplexed inductively coupled plasma etcher", J. Electrochemical Society, vol 146, 1999, p 339-349

16 F. Laermer, A. Schilp, K. Funk, and M. Offenberg "Bosch deep silicon etching: improving unifomity and etch rate for adveanced MEMS aplications", Proceedings of IEEE Micro Electro Mechanical Systems, Orlando (USA), 1999, p.211-216

17 P.-A. Clerc, L. Dellmann, F. Grétillat, M.-A. Grétillat, P. F. Indermühle, S. Jeanneret, P. Luginbuhl, C. Marxer, T. L. Pfeffer, G. - A. Racine, S. Roth, U. Staufer, C. Stebler, P. Thiébaud, and N.F. de Rooij "Advanced deep reactive etching: a versatile tool for microelectromechanical systems", J. Micromech. Microeng., vol 8, 1998, p 272-278

18 H. Jansen, M. de Boer, and M. Elwenspoek "The black silicon method VI: high aspect ratio trench etching for MEMS applications" Proceedings of IEEE Micro Electro Mechanical Systems, San Diego (USA), 1996, p.250-257

19 G. Engelmann, O. Ehrmann, J. Simon, and H. Reichl "Development of a fine pitch bumping process" Micro System Technologies 90, Springer-Verlag, Berlin (Germany), p. 435-440

20 S. Gernet, M. Koudelka, and N. F. de Rooij "Fabrication and characterization of a planar electrochemical cell and its application as a glucose sensor" Sensors and Actuators, vol. 18, 1989, p. 59-70

21 P. Thiébaud, N.F. de Rooij, M. Koudelka-Hep, and L. Stoppini "Microelectrode arrays for electrophysiological monitoring of hippocampal organotypic slice cultures" IEEE transactions on biomedical engineering, vol. 44, 1997, p. 1159-1163

22 O. Wolter, T. Bayer, and J. Greschner "Micromachined silicon sensors for scanning force microscopy" Journal of vacuum science and technology, vol B9, 1991, p. 1353-1357

23 C. Beuret, P. Niedermann, U. Staufer, and N. F. de Rooij "Fabrication of metallic probes by a new technology based on double molding" Microelectronic Engineering, vol. 41/42, 1998, p. 543-546

24 G. C. Fiaccabrino and M. Koudelka-Hep "Thin-film microfabrication of electrochemical transducers". Electroanalysis, vol. 10, 1998, p. 217-222

25 S. Roth, L. Dellmann, G.-A. Racine, and N. F. de Rooij "High aspect ratio UV photolithography for electroplated structures" Proceedings Micromechanics Europe, 1998, p. 105-109

26 P. Thiébaud, C. Beuret, M. Koudelka-Hep, M. Bove, S. Martinoia, M. Grattarola, H. Jahnsen, R. Rebaudo, M. Balestrino, J. Zimmer, and Y. Dupont "An array of Pt-tip microelectrodes for extracellular monitoring of activity of brain slices" Biosensors & Bioelectronics, vol. 14, 1999, p. 61-65

27 K. Y. Lee, N. LaBianca, S. A. Rishton, S. Zolghamain, J. D. Gelorme, J. Shaw, and T. H.-P. Chang "Micromachining applications of a high resolution ultrathick photoresist" J. Vac. Sci. Technol. B, vol. 13, 1995, p. 3012-3016

28 M. Despont, H. Lorenz, N. Fahrni, J. Brugger, P. Renaud, and P. Vettiger "High-aspect-ratio, ultrathick, negative-tone near-UV photoresist for MEMS applications" Proceedings of IEEE Micro Electro Mechanical Systems, Nagoya (Japan), 1997, p.518-522

29 R. C. Davis, C. C. Williams, and P. Neuzil "Micromachined submicrometer photodiode for scanning probe microscopy" Appl. Phys. Lett., vol 66, 1995, p. 2309-2311

30 G. Schürmann, P. F. Indermühle, U. Staufer and N. F. de Rooij "Micromachined SPM probes with sub 100 nm features at tip apex" accepted in Surface and Interface Analysis, 1999

31 A. B. Frazier, D. P. O'Brien, and M. G. Allen "Two dimensional metallic microelectrode arrays for extracellular stimulation and recording of neurons" Proceedings of IEEE Micro Electro Mechanical Systems, Fort Lauderdale 1993, p.195-200

32 H. Tabel, M. Takahashi, S. Hoshino, O. Niwa, and T. Horiuchi "Subfemtomole detection of catecholamine with interdigitated array carbon microelectrodes in HPLC" Analytical Chemistry, vol. 66, 1994, p. 3500-3502

4. Characterisations and measurements

The two main shapes of the three dimensional microelectrodes realised, the hillocks and the tips, were evaluated in order to determine their characteristics. Linked with the optical observations, electrical and electrochemical tests were first performed in order to have a set of criteria to predict their behaviours. Hippocampal slices of rats were cultured on the MEAs by using the long term organotypic culture by interface method and their histology studied. To illustrate the possibilities of applications of the devices, several electrophysiological tests will be described, as well as the measurement set-up which has to be adapted to the MEAs.

Part of the characterisations were accomplished at our institute, however the characterisations of impedance, the histology and the electrophysiological measurements were performed in several specialised research groups, with which we have closely collaborated. To begin with Dr Stoppini at University of Geneva (Switzerland), and then with the European project "*In vitro* neurotoxicology tests based on the coupling of brain slices to silicon microelectrode arrays", the experiments linked to the use of neurons were undertaken. In order to show the suitability of the realised MEAs, the main achievements obtained in these laboratories will be indicated in this chapter.

4.1. Meeeuremente of the electrodee geometry

Besides the position of the electrodes in the cultured slice, their surface area and their morphology are another two significant characteristics. The electrodes should be as small as possible to have a localised point of measurement or of

stimulation on the one hand. Their size should be at least comparable to that of the neurons. On the other hand, their surface has to be as big as possible to guarantee a sufficient coupling between the electrode and the tissue, that means a low impedance. A solution consists in the realisation of a rough surface, as long as this structure remains mechanically stable. Following this idea, the electrodeposited platinum hillocks were deposited introducing a certain surface roughness.

The geometrical surface of the planar electrode can easily be measured since it forms a circle with a diameter of 11 μm. The surface of the hillocks shape electrode can be approximated by a half-sphere of 40 μm in diameter and 20 μm in height. The platinum tips are approximated by a cone with a circular base of 15 μm in diameter and 20 μm in height. The platinum tips with only a small area opened at the top are also approximated by a cone with a circular base of 2.5 μm in diameter and 2 μm in height. The calculated geometrical surface areas of the electrodes are given in table 4.1.

These electrodes are observed by using the optical microscope and the scanning electron microscopy (SEM). This last method of observation does not ensure that the observed surface is platinum or if a remaining passivation layer covers it. The platinum can be easily determined, in the case of a flat structure, by an optical microscope or a conductivity measurement on a test structure by using needles probes. As for the tips, another test to determine the opening of

Table 4.1. Geometrical areas of the electrodes.

electrodes	surface
planar	95 μm^2
hillock	3770 μm^2
tip	505 μm^2
tip small	10 μm^2

the active area was developed. It consisted of the platinum plating process described in paragraph 3.4. for the hillocks shaped electrodes. Since the electrodeposition occurs only on the conductive surface, the electrode is highlighted and can be then observed by an SEM. This method were applied to both types of tip shaped electrodes which are shown in fig. 4.1. As a comparison, this test performed on a tip not yet completely open is shown in fig 4.2.

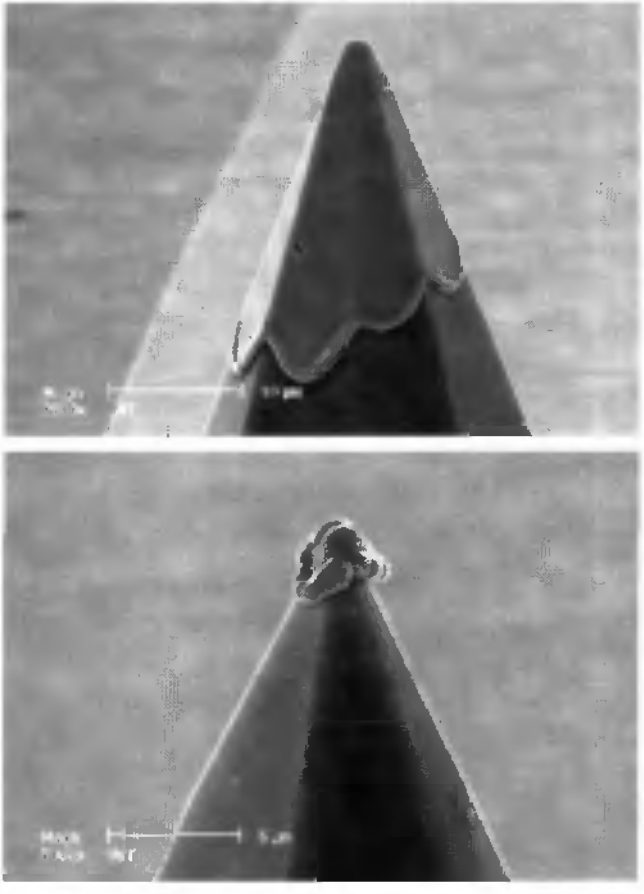

Fig. 4.1. Deposition of electroplated platinum on tip shaped electrodes of different sizes: standard (above) or small (bottom).

Fig. 4.2. Deposition of electroplated platinum on a not completely open tip shaped electrode.

Only five scans of the cyclic voltammetery should be used for this test of the platinum deposition. If the platinum layer is too thick, the stress can break the structure, like illustrated in fig. 4.3.

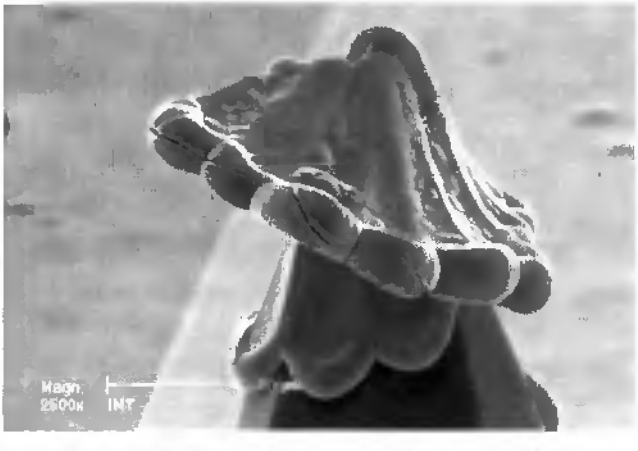

Fig. 4.3. Deposition of thicker electroplated platinum layer induces breaking of this layer.

The poor adhesion of such a platinum layer is a certain limitation to the use of these electroplated tips for electrophysiological measurements. however, this process allows, to increase the roughness of the electrodes and thus to decrease their impedance while maintaining the shape of a 50 µm high tip.

4.2. Impedance measurements

The impedance of the electrode interface during an electrophysiological measurements, can be assumed to be the one obtained with an impedance measurement in an electrolytic solution with an adequate composition [1]. For a classical electrode, as presented in paragraph 1.2., ended by a fine opening of a glass capillary and filled with a saline solution, the coupling with the extracellular fluid results in a liquid - liquid interface. That is why the impedance can be ohmic with a resistance of about 100 MΩ for an aperture of 30 nm like shown in fig. 1.1. In the case of a metallic electrode, another mode of coupling occurs. At the interface, an electrical double layer is formed by the electrons in the metal and by the ions close to its surface, resulting in a capacitive component. To represent that, the impedance of a platinum electrode is modellised by a resistance Re in parallel with a capacity Ce with changing values with the frequency. A high impedance value of the electrode causes an attenuation and the complex aspect of these electrodes results in a filtering effect on the measured signal. Thus the impedance values have to be known to evaluate their effect on the measurements; in particular, a sufficient signal to noise ratio should be obtained to analyse the data. Another important point is that the characteristics have to be the same for all the electrodes embedded on the chip, to allow the comparison of their results. For the electrical stimulation of the cultured neurons, a low impedance allows a better charge delivery for a given excitation voltage.

To measure these impedances, the MEAs were immersed in a physiological solution (NaCl 135 mM) with a reference electrode. The resistance of this electrode, of the metal tracks, and of the electrolyte is considered as negligible. These experiments, performed by the Prof. Grattarola's group, Department of Biophysical and Electronic Engineering, University of Genoa (Italy), were based on a lock-in amplifier (EG and G instruments 5110) connected to an external function generator (HP 8116A) and to a low-noise switching matrix system (Keithley 7074) which allowed an easy multiplexing of the output signals. All the instruments were controlled by a personal computer via a standard IEEE 488 interface. The measurements were performed by exciting each platinum electrode with small sinusoidal waves (20-200 mV in amplitude) and by sweeping the frequency from 200 Hz to 5 kHz. Output values from lock-in amplifier were the module and the phase respectively. They were translated into the module and the phase of the electrode impedance by compensating the capacitance of cables and connectors which was, in this case, of about 500 pF. Fig. 4.4. shows the impedance measurement for hillock shaped electrode. The plotted results indicate the average value of the 30 microelectrodes of a given array, the error bars representing the differences between the electrodes.

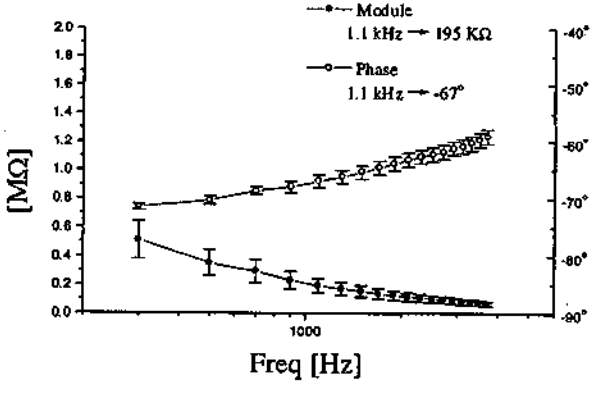

Fig. 4.4. Impedance as a function of the frequency of hillock electrodes (courtesy of Prof. Grattarola's group).

The electrodes show a decrease of impedance with frequency, but a relatively constant phase angle. Thus, at low frequency the impedance is higher resulting in a instability for DC measurements. In the literature, the values at a frequency of about 1 kHz corresponding to the time scale of an action potential are usually given. Therefore, the measured impedance of all the electrode shapes: tip, tip with a smaller area, planar, and hillocks is also given for about the same frequency on fig. 4.5. As expected, the impedance is linked to the surface area and the surface morphology of the electrodes. The hillock shaped electrode deposited by electroplating, with its large surface and its roughness, presents the best characteristics for signal transmission with the lowest impedance module. The lower value of the phase can be explained by the roughness like already described in the literature [2, 3]. The small surface and low roughness of the tip shaped electrodes results in a higher impedance value. This value is considered as too high for the tips with a small open area. The open area of the electrode is very similar, in particular among the electrodes of one chip. This is demonstrated by the homogeneity of the impedance values for these electrodes. The same is observed with the hillock shaped electrodes when the platinum is deposited at the same time on all the electrodes. This characteristic allows the evaluation of the activity of the measured neurons by ensuring similar experimental conditions for each signal.

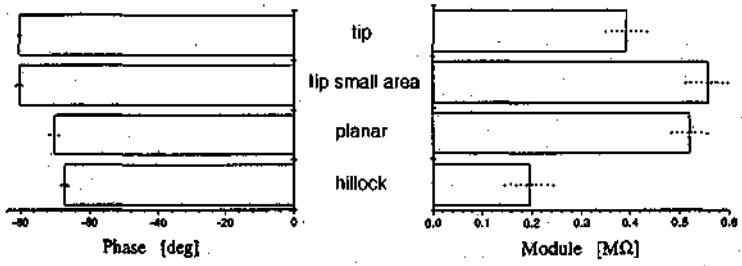

Fig. 4.5. Impedance at a frequency of 1.1 kHz of the different shapes of electrodes (courtesy of Prof. Grattarola's group).

Unfortunately, during the culturing of slice, the microelectrodes are affected by a dirtying of the surface and by the reaction of the tissue against the metal [2]. This results in an increase of the impedance such as for instance measured on the hillock electrodes and illustrated in fig. 4.6. Before the measurement the electrodes were cleaned accordingly the following procedure: rinsed with distilled and deionized water, then with NaOH 0.1 M, finally again with distilled and deionized water.

4.3. Electrochemical meaasurements

The quality surface of the microfabricated platinum electrodes can be verified by using electrochemical tests. During the fabrication process, the steps following the platinum deposition can deteriorate its surface. Interdiffusion of the atoms, from the tantalum adhesion layer to the electrodes surface, can occur during the high temperature process of the LPCVD silicon nitride top

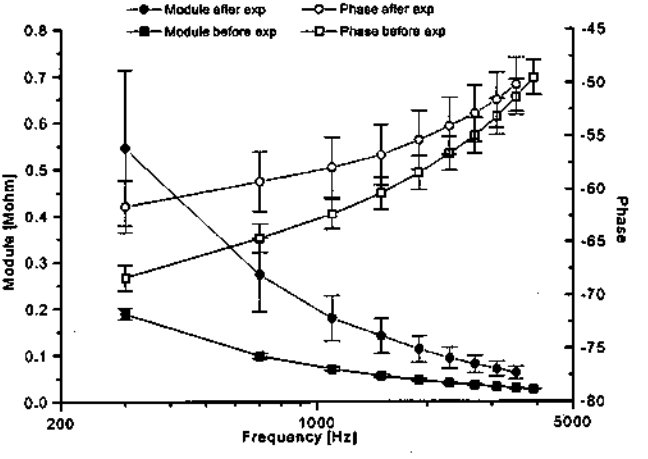

Fig. 4.6. Impedance before and after electrophysiological experiments on hillock shaped platinum electrodes (courtesy of Prof. Grattarola's group).

passivation deposition. Also the redeposition during the plasma etching of this passivation layer, or an insufficient cleaning of the photoresist can result in covering of the electrodes.

Cyclic voltammetry in H_2SO_4

The quality of the thin-film platinum can be analysed by observing the signal of a cyclic voltammetry, and compare it with the voltammogram of a bulk platinum electrode. This signal is linked to the number of reaction sites on the surface for each crystalline plans of the platinum [4]. The performed experiment is identical to the one presented in paragraph 3.4. as the pre-treatment of the platinum electrodes before platinum plating. It consists in a cyclic voltammetry in a 1M H_2SO_4 solution with a voltage scan from -0.25 V to about 1.5 V versus SCE, at 100 mV/s. The voltammograms of two types of platinum, namely the evaporated thin film electrodes and the electroplated hillocks are shown in fig 4.7. The electroplated platinum has better characteristics because no more technological operations were performed on the platinum surface. On planar electrodes, an improvement of the signal is observed after each voltage scan showing thus a cleaning process of the platinum surface. The real surface of platinum can be obtained from the voltammogram and can be compared to the geometrical surface measured in paragraph 4.1. The ratio of the real surface to the geometrical surface defines the roughness factor f_r. The method used to evaluate the real surface is based on the measurement of the charge associated with the desorption of a monolayer of hydrogen on the microelectrode [5]. This value is obtained by integrating the voltammogram curve in the hydrogen desorption part. The real surface is then calculated considering that the charge per surface area associated with the desorption of a monolayer of hydrogen corresponds to 210 $\mu C/cm^2$. For the hillock shaped electrodes, the integral (measured from -225 mV to 200 mV at a scan rate of 100 mV/s) gives a charge of 0.11 μC for each

electrode and thus their roughness factor f_r is about 14. For the evaporated platinum f_r is between 2-3 [5]. These results are summarised in table 4.2.

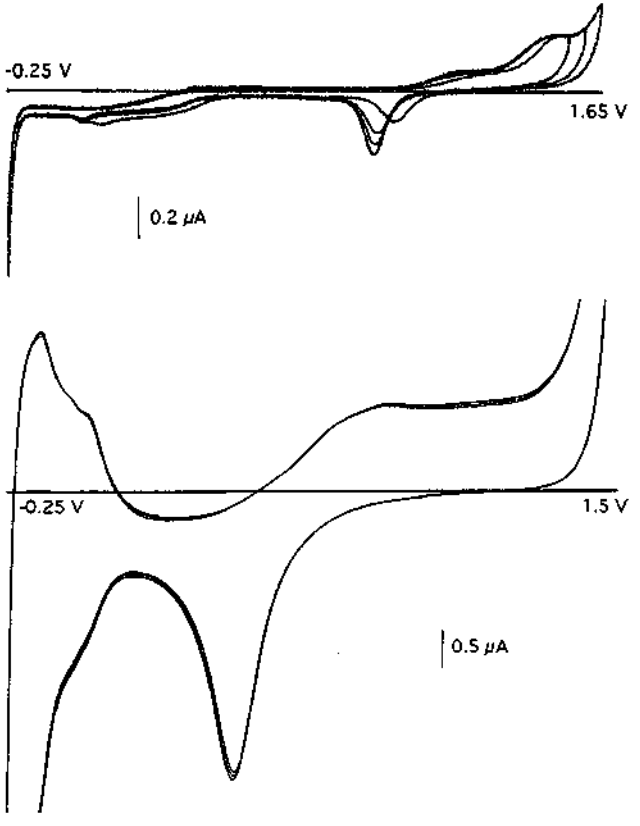

Fig. 4.7. Voltammogram of the evaporated platinum measured on 30 planar electrodes (above) and 30 electroplated platinum (bottom) in a non deoxygenated 1M H_2SO_4 solution.

Table 4.2. Roughness factor of the electroplated and evaporated platinum.

platinum	f_r
electroplated	14
evaporated	2-3

Cyclic voltammetry in KCl/ferro-CN

The electrochemical behaviour of the different microelectrodes was examined for the oxidation of ferrocyanide (ferro-CN). These tests are made by cyclic voltammetry in a 1M KCl solution containing 10 mM ferro-CN with a voltage scan from 0.1 V to 0.9 V versus SCE, at 50 mV/s. The three electrode types were measured and the results are shown in fig. 4.8. A quasi-steady-state currents were obtained for all the electrodes. The planar electrodes show a slightly higher resistive aspect because of their high impedance. The electroplated platinum behaves in a similar way to a macro electrode. The resulting current values after deduction of the background current measured before the ferro-CN addition are indicated in table 4.3.

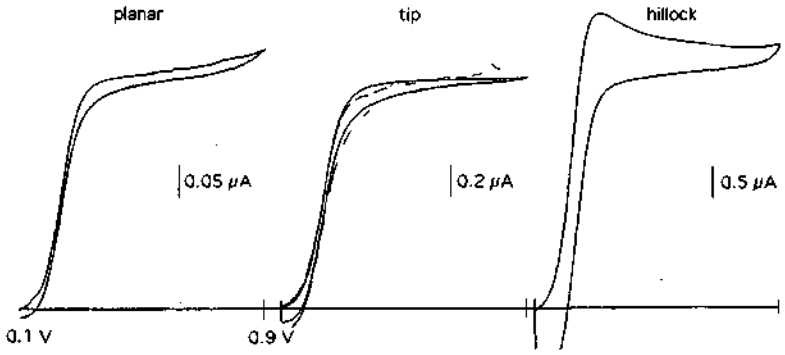

Fig. 4.8. Voltammograms of 30 electrodes of each type in 1M KCl solution containing 10mM ferro-CN at 50 mV/s (dashed line 100 mV/s).

Table 4.3. Currents for one electrode in 1M KCl solution containing 10mM ferro-CN after deduction of the background current.

electrode	current
planar	11 nA
tip	48 nA
hillock	140 nA

4.4. Culturea on silicon perforated aubstrate

The perforated substrate was designed to be biocompatible and adapted for the organotypic culture by interface, like described in paragraph 2.1. A survival of several weeks has to be obtained in order that the young tissue becomes mature. A culture is considered as organotypic if the morphology, the synaptic circuitry, the neurotransmitter receptor distribution and the electrophysiology are similar to these *in vivo*. It has been established that the hippocampus slices of rats keep these properties in conventional organotypic culture by interface [6, 7, 8]. The electrophysiology will be described in the next paragraph. The other aspects are analysed by the histology of a cultured slice and the use of several markers. To ensure the survival of a slice on the MEA, several tests were performed, first in the group of Dr. Stoppini, in the Department of Pharmacology, University of Geneva (Switzerland), and then in the group of Prof. Zimmer, in the Department of Anatomy and Cell Biology, University of Odense (Denmark). The observations of Dr. Stoppini established that the minimum porosity required is 13 % and that the holes diameter has to be smaller than 40 μm. Actually, if the holes are too big, a large amount of tissue slides inside them. Prof. Zimmer performed a comparative experiment, described in detail in [9], by culturing slices on the microfabricated device and at the same time on the regular substrates of a Millicell-CM membrane from Millipore. Thus, the tissues cultured on both substrates were exposed to the same experimental conditions. The histological organisation can be verified by using a microscope during all the time of culturing and afterwards. The fig. 4.9. shows a photograph of a slice after 2 weeks of culturing, sectioned in three parts, to illustrate how the tissue adapted itself to the perforated substrate.

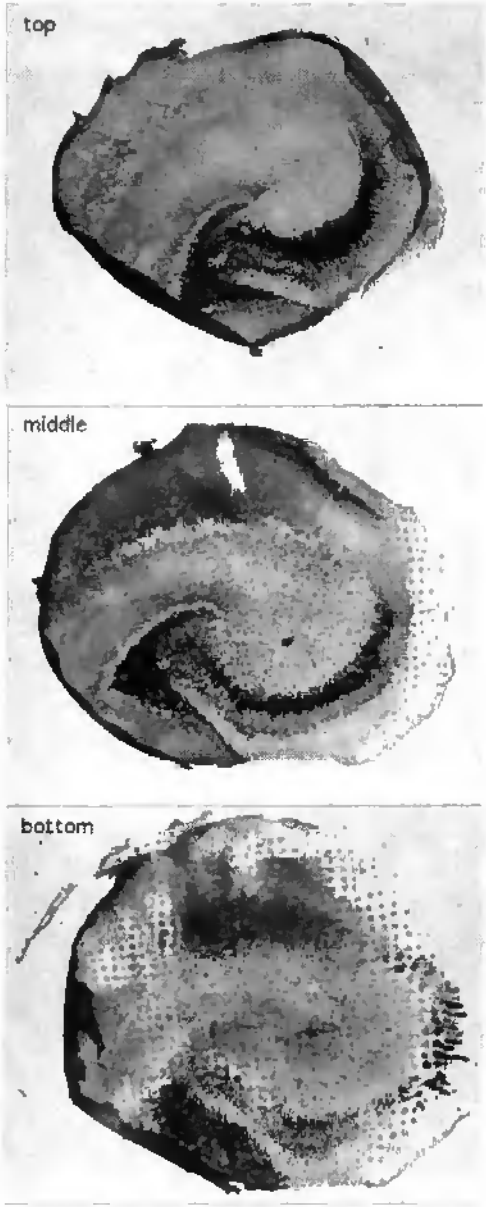

Fig. 4.9. Photograph of a slice separated in 3 layers after 2 weeks of culturing on the perforated substrate (courtesy of Prof. Zimmer's group).

The structure of the rat's hippocampus, such as described in paragraph 2.6., can be recognised. A small proportion of the tissue is placed inside the hole but does not affect the viability of the neurons, as demonstrated in the following experiments.

Chemical markers were used to highlight several aspects of the tissue. For instance, propidium iodide is a non-toxic compound which becomes fluorescent when bonded on nucleic acid of damaged cells. By that mean, the necrosis can be observed and also, after having killed all the neurons, their numbers in the culture can be evaluated. The fig. 4.10. shows these results. The number of dead neurons was very low in all cultures, nevertheless, a cellular degeneration was sometimes detected in the central part of the tissue. This degeneration is found more often in cultures made with the classical method than on the MEA.

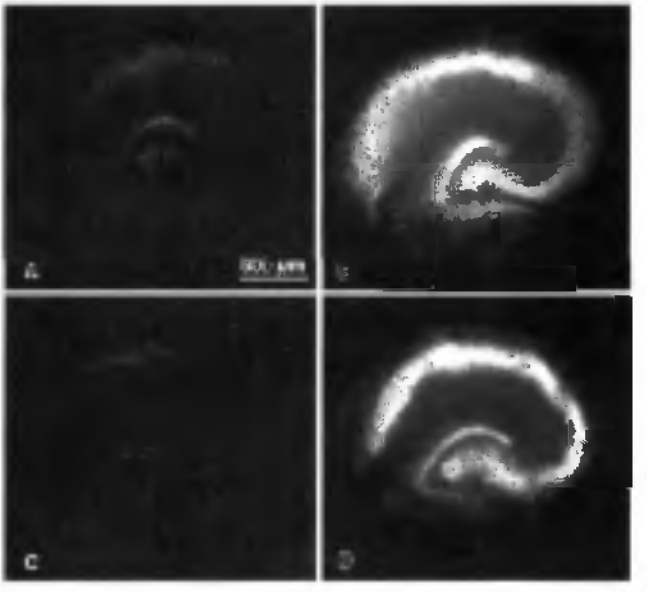

Fig. 4.10. Fluorescent microscope digital images of PI uptake after 4 weeks in culture on Millicell membrane (A, B) and on MEA (C, D), before (A, C) and after (B, D) that the neurons were killed (from [9]).

This fact can be explained by the difference of thickness of the tissue. Actually, the slice cultured on the microfabricated chip tends to flatten slightly more rapidly, decreasing the distance for the gas exchanges. Another aspects conceming some specific elements of the cultured cells were analysed by using corresponding staining methods: the general cytological organisation, the fibres connections, the dendritic parts of the neurons and the glial cells. The conclusion is that the organotypic organisation is verified and that except for the thickness, the cultures on Millicell membrane and on MEA show identical characteristics.

Conceming the maximum time of survival, in these experimental circumstances, slices were kept in good biological conditions up to 8 weeks. The possibility of cleaning the devices, based on the use of soluene (an enzymatic solution) and concentrated acetic acid, were also developed in order to allow the re-use of the structures. Unfortunately this method cannot be applied when the chip is encapsulated because the support does not bear this treatment. In summary, all these results have demonstrated the biocompatibility of the MEA and its suitability for long term organotypic culture by interface.

4.5. Electrophysiologicsl messuremsnts

In order to test the possibility to stimulate and to record the electrical activity of the cultured neurons by the different electrode shapes, a series of electrophysiological measurements was performed. These tests focused mainly on the results obtained with the hillock shaped and tip shaped electrode. Due to the low interest in planar electrodes, only a few experiments were undertaken. Some results on the same type of electrode, also fabricated in our laboratory, are presented for the same conditions of the culture in [10]. The phenomena involved in the electrophysiological measurements are explained in chapter 2 and in the annexe.

Set-up

Before these measurements, an adapted set-up for the MEA has to be realised and is approximately the same for all the tests. In order to make the electrical connections, the silicon chip is glued on a printed circuit board (PCB), bonded, and encapsulated with epoxy (Araldite AY105/HY991, from Ciba). The dimensions of this support are 5.4 cm x 7.5 cm. A bottom chamber containing the nutritive solution, acts as a microperfusion chamber. The medium reaches the culture through a hole in the PCB, and through the perforated array. A perfusion connected to this chamber refreshes the solution. An upper chamber is placed on the PCB to prevent the slice from drying. This chamber is closed by a transparent cover plate to allow the observation of the tissue. A scheme of this set-up is shown in fig. 4.11. The bottom chamber can be laid on a heater to maintain a temperature of 37 °C in the system. A 100 % humidity warm air, extracted from this heater, can also be connected to the upper chamber. These temperature and humidity control enhanced the viability of the slice during the measurement. Between the measurements sessions the system is stored in an incubator with the micro perfusion chamber in a 5% CO_2 atmosphere. The nutritive solution supply has to be carefully adjusted to guarantee a sufficient

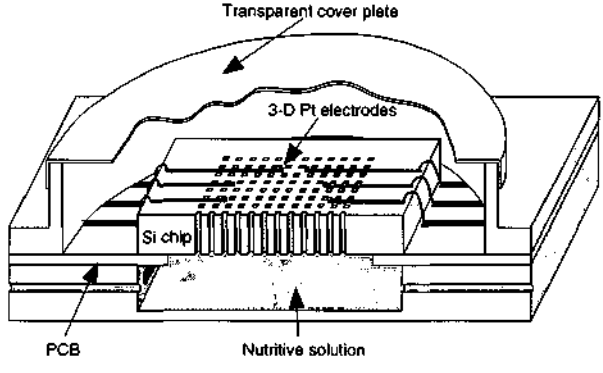

Fig. 4.11. Schematic view of the measurement set-up (from [11]).

influx to the tissue. Bubbles of air which can block some of the holes have also to be prevented. The handling of the fluidic part represents an important part of the experimental set-up and must be carefully adjusted. So far, a long term viability was not yet achieved in these experiments, even though this objective was achieved on a single chip in an incubation chamber, as described in the previous paragraph.

Hillock shaped microelectrodes.

The tests on these electrodes were performed by the group of Dr. Stoppini, in the Department of Pharmacology, University of Geneva (Switzerland) and are described in [11]. Prior to use, the chip and the set-up were sterilised with ethylene oxide. The tissue consists of hippocampus slices dissected out from seven days old Wistar rats. After 10-15 days of normal culturing in a petri dish, the slices were transferred onto the perforated MEA. In some experiments the tissue was resting on a Millicell-CM supporting membrane disk, while in others, the tissue was directly in contact with the substrate. Slice cultures were positioned so that two microelectrodes, located in the CA3 region, could be used for stimulation, and six electrodes, located in the CA3-CA1 area, for recording. Fig. 4.12. shows a photograph of the MEA with a so placed hippocampal slice. All the signals were amplified by an electronic circuit under computer control. The stimulation pulses of 0.8-1.2 V (of about 1 μA) and of a duration of 1 ms were delivered at 30-60 s intervals. Representative evoked potentials of six electrodes located in the CA1-CA3 area are shown in fig. 4.13. The part (A) shows the results obtained when the slice culture was resting on the supporting membrane while in part (B) the culture was in direct contact with the array. It should be noticed that in both cases large signal amplitudes and a good signal to noise ratio were obtained. The possibility to record field potentials with a signal to noise ratio between 6:1 and 10:1 when the culture is resting on the supporting membrane is particularly interesting. It opens the

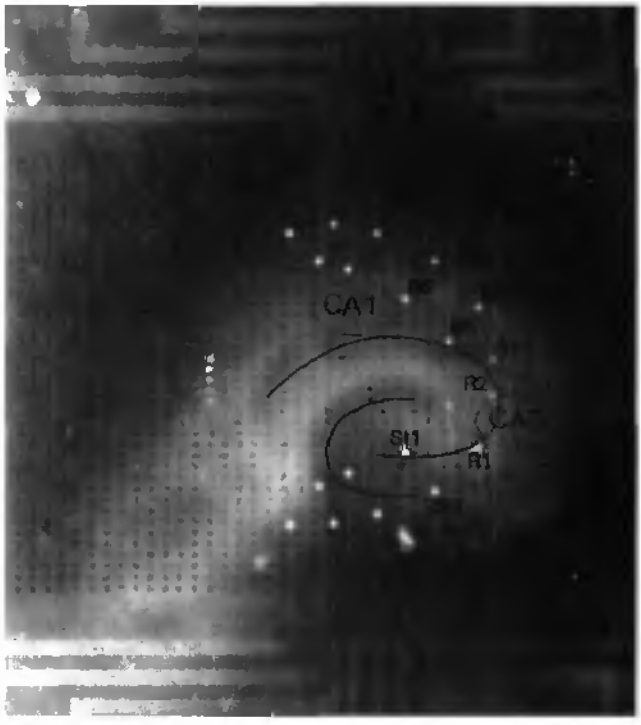

Fig. 4.12. Photograph of a hippocampal slice on the MEA with a typical location for the stimulation and recording electrodes (from [111]).

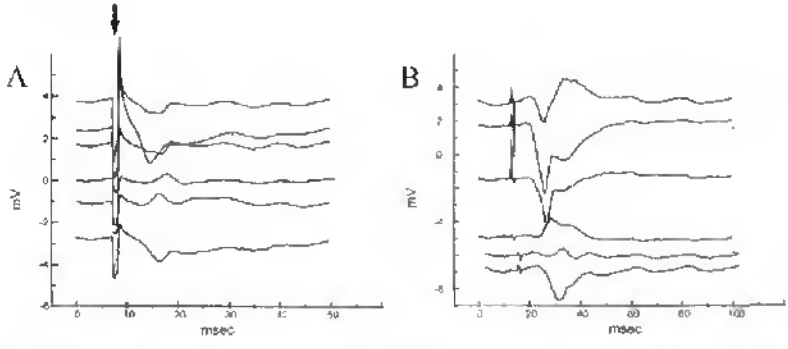

Fig. 4.13. Example of recordings on hillock shaped MEA obtained with (A) and without (B) the membrane supporting the tissue. The arrow indicates the stimulation artefact (from [111]).

opportunities to manipulate the tissue slice for precise positioning or to remove it without tissue injuries with the tweezers and without breaking the fragile hillocks electrodes. Field potentials could be detected for three days at room temperature with a continuous stimulation at 1/60 Hz like shown in fig 4.14. but up to eight days of recording was achieved when the set-up was placed in the incubator between the recording sessions. This survival time was limited by the non optimised conditions for the medium supply, resulting in a drying of the slices.

In order to confirm the viability and functionality of the slice culture, experiments with a neuroactive molecule has been performed. By the perfusion, Picrotoxin 10 μM was injected during 10 minutes. Synchronous neural activity lasting for less than 1 minute could be observed in fig. 4.15.(B) and 4.15.(C) then replaced with characteristic arrhythmic bursts in fig 4.15.(D) which have disappeared after one hour wash.

These measurements demonstrate that the hillock shaped microelectrodes, due to their shape and low impedance, allow good electrical connections with the nervous tissue to be achieved.

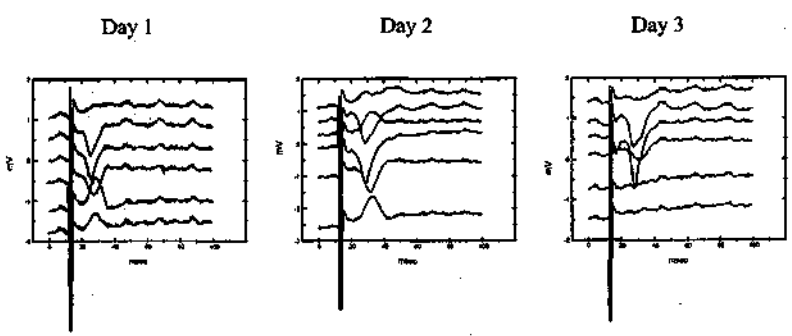

Fig. 4.14. Representative responses on hillock shaped MEA recorded during three days (from [11]).

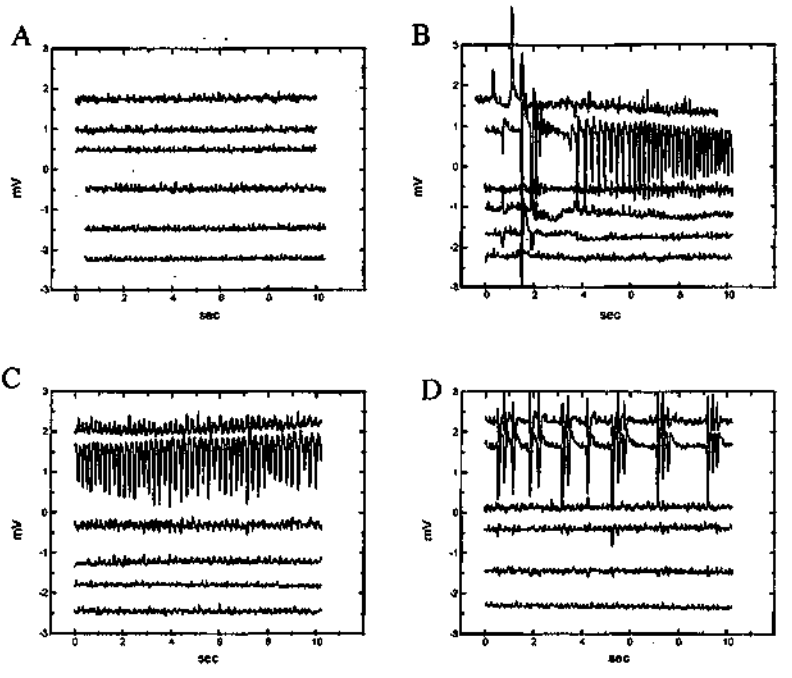

Fig. 4.15. Spontaneous field potentials recorded on hillock shaped MEA before (A) and after (B) perfusion of Picrotoxin. A stimulation paradigm triggers rhythmic field potentials (channel 1 and 2 in (C)) then replaced by arrhythmic bursts (D) (from [11]).

Tip shaped microelectrodes.

Several research groups were involved in the tests on these electrodes. The group of Dr. Jahnsen, in the Department of Medical Physiology, University of Copenhagen (Denmark) in collaboration with the group of Prof. Zimmer, in the Department of Anatomy and Cell Biology, University of Odense (Denmark) and the group of Dr. Balestrino, in the Department of Neurology, University of Genoa (Italy), in collaboration with the group of Prof. Grattarola in the Department of Biophysical and Electronic Engineering, University of Genoa (Italy). This evaluation is now in progress but some preliminary results could

already be obtained [12]. After the MEAs integration in the microperfusion chamber, electrophysiological measurements have been performed on hippocampal slices of rats. A representative example of recordings after 17 days in culture is shown in fig. 4.16. A tungsten external electrode was used to stimulate in the CA3 region and the summed action potentials were recorded in the CA1, CA3 and dentate gyrus region. A measurement on a conventional glass electrode was also performed to allow the comparison with the microelectrodes.

The capability of the platinum tip to record anoxic depolarisation was also investigated. This is a slow spreading depression-like potential that has been linked to hypoxic irreversible damage [13]. For this aim, the extracellular potentials during hypoxia of the slice were recorded. The hypoxia was obtained

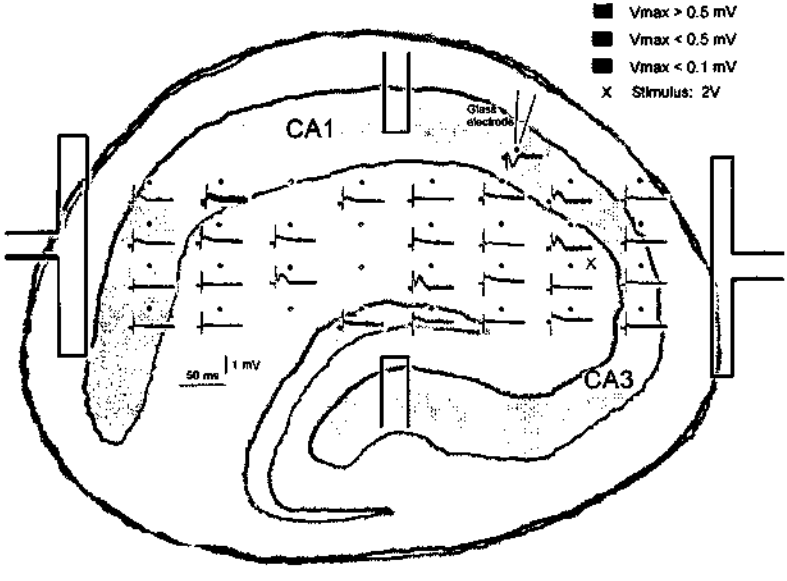

Fig. 4.16. Representative responses on tip shaped MEA and on a classical glass electrode. The four electrodes without signal are not connected (courtesy of Dr. Jahnsen's group).

by completely replacing the oxygen with nitrogen in the gas phase. After the start of hypoxia, a voltage deflection is detected that could be identified, based on its latency and shape as anoxic depolarisation. Although electrical noise and drift of the baseline were present, the sudden depolarisation of anoxic depolarisation can be seen in fig. 4.17.

This experiment illustrates the difficulty to measure a DC signal with a high impedance metallic electrode. The capacitive aspect of these electrodes induces an instability of the baseline. A lower impedance value, like that of the electroplated microelectrodes, or a pure resistive contact like with the classical glass electrodes, should improve this type of measurements.

Despite this high impedance, faster biological events than anoxic depolarisation, such as presented in fig. 4.16., can be detected by the tip shaped microelectrodes. Moreover these electrodes present interesting additional advantages compared to the hillocks: their mechanical solidity and their penetration into the tissue allowing more localised measurements to be achieved.

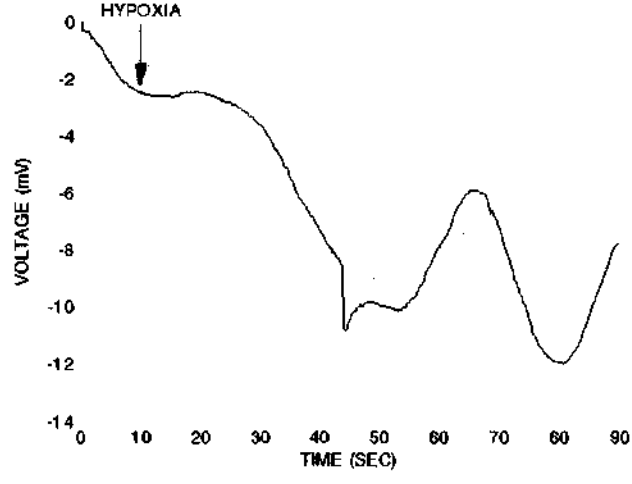

Fig. 4.17. Anoxic depolarisation measured on tip shaped MEA (from [12]).

1 S. J. Carter, C. J. Linker, T. Turkle-Huslig, and L. L. Howard "Comparison of impedance at the microelectrode-saline and micro-culture medium interface" IEEE transactions on biomedical engineering, vol. 39, 1992, p. 1123-1128

2 E. T. McAdams, J. A. McLaughlin, and D. S. Holder "Neurosensors: a review of some fundamental electrode parameters" 14th annual international conference of the IEEE engineering in medicine and biology society, Lyon (France), 1992

3 M. Hyland, J. A. McLaughlin, D. -M. Zhou, and E. T. McAdams "Surface modification of thin film gold electrodes for improved *in vivo* preformance" Analyst, vol. 121, 1996, p. 705-709

4 S. Gernet, M. Koudelka, and N. F. de Rooij "Fabrication and characterisation of a planar electrochemical cell and its application as a glucose sensor", Sensors and Actuators, vol. 18, 1989, p. 59-70

5 S. Gernet "Realization of a miniaturized planar amperometric glucose sensor for biomedical applications", Thesis dissertation, University of Neuchâtel, 1990

6 L. Stoppini, P.-A. Buchs, and D. Muller "A simple method for organotypic cultures of nervous tissue", journal of neuroscience methods, vol. 37, 1991, p. 173-182

7 B. A. Bahr, "Long-term hippocampal slices: a model system for investigating synaptic mechanisms and pathologic processes", journal of neuroscience res., vol. 42, 1995, p. 294-305

8 S. Fennirich, H. Stier, K.-J. Föhr, D. Rey, J.-F. Ghersi-Egea, and B. Schlosshauser "Organotypic rat brain culture as in vivo-like model system", methods in cell science, vol. 18, 1996, p. 283-291

9 H. Jahnsen, B. W. Kristensen, P. Thiébaud, J. Noraberg, B. Jakobsen, M. Bove, S. Martinoia, M. Koudelka-Hep, M. Grattarola, and J. Zimmer

"Coupling of organotypic brain slice cultures to silicon-based arrays of electrodes" Methods: a companion to methods in enzymology, vol. 18, 1999, p.160-172 or http://www.idealibrary.com

10 A. Gisiger, P.-A. Clerc, S. Jeanneret, N. F. de Rooij, and M. Koudelka-Hep "Electrode array on porous membranes for biological preparations" The fifth international meeting on chemical sensor, Rome, 1994, p.205-208

11 P. Thiébaud, N.F. de Rooij, M. Koudelka - Hep, and L. Stoppini "Microelectrode arrays for electrophysiological monitoring of hippocampal organotypic slice cultures" IEEE transactions on biomedical engineering, vol. 44, 1997, p. 1159-1163

12 P. Thiébaud, C. Beuret, M. Koudelka-Hep, M. Bove, S. Martinoia, M. Grattarola, H. Jahnsen, R. Rebaudo, M. Balestrino, J. Zimmer, and Y. Dupont "An array of Pt-tip microelectrodes for extracellular monitoring of activity of brain slices" Biosensors & Bioelectronics, vol. 14, 1999, p. 61-65

13 M. Balestrino "Pathophysiology of anoxic depolarisatin: new findings and a working hypothesis" Journal of neuroscience methods, vol. 59, 1995, p. 99-103

5. Conclusions

In the course of this work, several microelectrode arrays were fabricated in order to be used for monitoring of the electrical activity of the neurons in organotypic slice culture by interface. One aspect which was developed, was the perforation method to obtain a mechanically stable porous substrate required for this kind of culture. The viability tests with brain slices have demonstrated that the selected design and technology, as well as the materials, were appropriate to perform long term cultures on these devices. The second research aspect consisted of the improvement of the coupling of the electrodes with the neurons cultured in thick slice, in particular the organotypic cultures. To achieve this, three dimensional electrodes were build in order to decrease their impedance value and to allow a better location in the tissue. Two platinum three dimensional electrodes were fabricated: electroplated hillocks and tips. For thick tissues, the tip shape electrodes represent an interesting tool compared with the planar electrode now commercially available because they are localised inside the tissue, close to the soma of the cultured neurones. If a lower impedance electrodes are needed, the hillocks can be used.

From a technological point of view, the originality of these devices consists of the combination of high aspect ratio structures both through the substrate and above the surface. Silicon deep reactive ion etching together with silicon anisotropic wet etching associated to thick photolithography were used in order to fabricate these microelectrodes arrays.

The development of these devices has involved a lot of interactions between very different fields and this aspect was a critical point for the success of this research. The coordination and the exchanges with several laboratories have resulted in a very efficient collaboration allowing these devices to be realised and evaluated.

Annexe: Principles of neural communication

The potential changes measured by the microelectrode arrays are caused by ions' exchanges produced by the neurons during either their normal activity or artificially evoked. This chapter will first shortly define the morphology and explain the bases of signals transmissions between neurons, especially from an electrical point of view. More extended information can be found in the related literature [1, 2, 3, 4, 5].

A.1. Neuron description

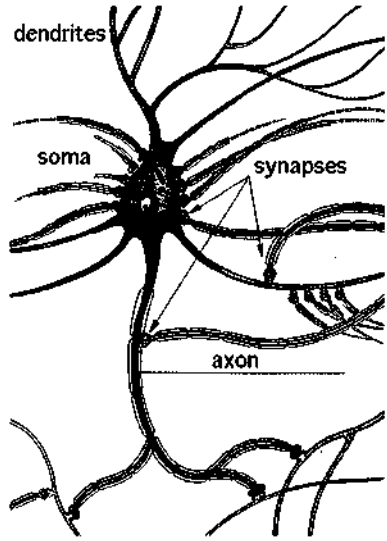

Fig. A.1. Scheme of a neuron (modified from [6]).

Like all the cells of the organism, neurons consist of the following elements. The membrane separate the inside and the outside and enclose several structures like the nucleus, which contains the chromosomes, in a fluid called the cytosol. The neuron has specialised parts shown in figure A.1. The region around the nucleus is called cell body or soma. From the soma the dendrites and the axon radiate away. There is normally a single axon which extend much further than dendrites. If the axon divides itself in different directions these are called axons collateral. The axon splits at its extremity in many branches and comes in contact with other neurons on places named synapses. The neuron normally receives signals on its dendrites or on its soma. These inputs are integrated, a response is generated, conducted through the axon to the synapses and finally transmitted to others neurons by using chemical messengers, the neurotransmitters. The cytosol and the extracellular fluid contain ions in a very different concentration. The most important ones are potassium (K^+), sodium (Na^+), calcium (Ca^{2+}), and chloride (Cl^-). Their concentrations are indicated in the table 1. Ion channels are distributed through the membrane. They are selectively permeable to ions and are gated by voltage and chemical components. Through these channels the diffusion produced by the concentration gradient results in a net movement of charges. An electrical field is then produced and compensate the diffusion force in order to reach the

Table 1. Ionic concentrations (from [4]).

ions	extracellular fluid outside	cytosol inside	Ratio outside/inside
K^+	5 mM	100 mM	1:20
Na^+	150 mM	15 mM	10:1
Ca^{2+}	2 mM	0.0002 mM	10 000:1
Cl^-	150 mM	13 mM	11.5:1

equilibrium and finally a double layer of ions is formed. The resulting potential E_{ion} for one particular ion is described by Nemst equation [7]:

$$E_{ion} = 2.303\frac{RT}{zF}\log\frac{ion_{out}}{ion_{in}}$$

where:

R: gas constant

T: absolute temperature

z: charge of the ion

F: Faraday's constant

$ion_{out/in}$: ionic concentration outside/inside the cell

The membrane is essentially permeable to potassium (E_{K^+} = -80 mV) and sodium (E_{Na^+} = -62 mV) but the conductivity of K^+ channels is 40 times higher than Na^+ channels The resulting membrane equilibrium potential V_{eq} is -65 mV with respect to the extracellular fluid and can be calculated by the Goldman equation modified by Hodgkin and Katz [1]:

$$V_{eq} = 2.303\frac{RT}{zF}\log\frac{P_K\ K^+_{out} + P_{Na}\ Na^+_{out}}{P_K\ K^+_{in} + P_{Na}\ Na^+_{in}}$$

where:

P_{ion}: relative permeabilities of one ion

The membrane voltage remains so long as the channels have the same conductivity and the ions' gradients are stable. A depolarisation takes place if a perturbation modifies this equilibrium and the membrane becomes less negative; an hyperpolarisation if more negative.

The difference of ions' density is maintained by the active action of a membrane-associated protein: the sodium-potassium pump which moves these

ions against their concentrations' gradients. During this process, the amount of charges remains the same inside and outside the cell. The sodium-potassium pumps consumes energy by the transformation of adrenosine triphosphate (ATP) into adrenosine diphosphate (ADP). The ATP is produced inside the cell by using oxygen and food derivatives [8]. If there is a lack of oxygen in the tissue, the ATP is no more fabricated. As a consequence the sodium-potassium pump cannot regulate the ratio of potassium concentration between the extracellular fluid and the cytosol. Thus, a diminution of the value of the membrane voltage is observed during this process which is called anoxic depolarisation. An example of this phenomena is given in paragraph 4.5.

The electrical properties of the membrane can be modelised by an electrical circuit shown in fig A.2. In this scheme, Rc represents the resistance through the membrane (via the channels) under the voltage Vc, Cm the capacitance of the double layer and Ri the longitudinal resistance inside the cell. During a depolarisation or an hyperpolarisation, an ionic flux is added. Thus, a net current Im is induced through the membrane, and can be put on the equivalent circuit.

Around the neurons, glia cells play different roles. For instance in the central nervous system (CNS), astrocytes act as support and they regulate the extracellular fluid composition. Another type is the oligodendroglia which produce a myelin sheath wrapped around some axon to isolate it. The uncovered places in between the myelined parts are called node of Ravier.

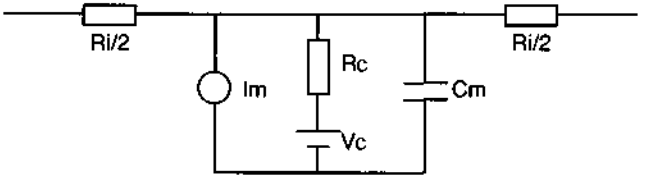

Fig. A.2. Equivalent circuit of the neurons' membrane (modified from [3]).

A.2. The action potential

The axon transports information by means of action potential which consists of pulses of the membrane potential going over the axon axis. This potential which is at rest -65 mV increases up to about +40 mV, then decreases up beyond the initial value before to stabilising. Thus, an action potential can be divided into three phases as shown in the figure A.3. These modifications are caused by changes in the conductivity of K^+ and Na^+ channels which are voltage-dependant:

1) First the raising phase: the pulse is trigged when the membrane potential reaches a threshold of about -40 mV. At that potential the Na^+ channels open, and pushed by a important voltage, sodium rushes inside the cells causing a depolarisation.
2) Then, two factors contribute to the falling phase: the Na^+ channels hermetically close until the membrane voltage returns to threshold, and the K^+ channels, trigged at the same time than Na^+ channels, open with about 1 ms delay allowing potassium to rush outside the cell.

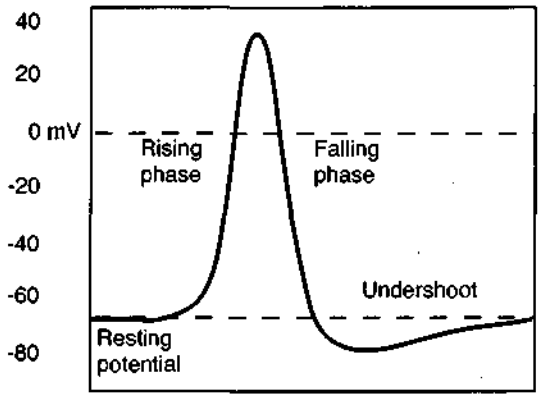

Fig A.3. Scheme of an action potential (modified from [4]).

3) So long as the K^+ channels do not recover their normal conductivity, about 2 ms after the beginning of the action potential, the membrane is hyperpolarised, forming the undershoot.

When the membrane is depolarised at one point, the threshold is reached at the next position just ahead, starting another action potential. By that mean the action potential propagates in the axon like illustrate in fig. A.4. The inactivation of Na^+ channels after the depolarisation avoids that the propagation goes back to the soma. The propagation velocity depends on how far the incoming sodium ions can provoke a new action potential. The membrane has many open pores through which the ions can flow out, introducing a competition between the ions progression and this leakage. To circumvent that, the axon should either be larger in diameter or have a myelin sheath, the actions potentials jumping from one node of Ranvier to the next one. A typical value of the velocity can be assumed at 10 m/s, since the duration of an action potential is about 2 ms, a size in the order of 2 cm can be calculated. The aspect of an action potential remains the same, only the time and the rate when it occurs contain informations. After having travelled through the whole axon the action potential arrives at the synapses.

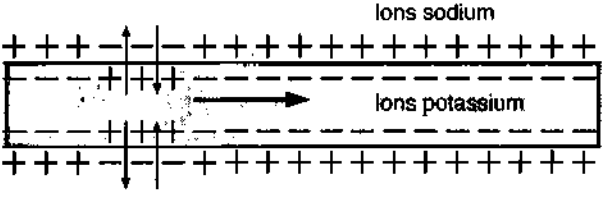

Fig A.4. Movements of the ions during the propagation of an action potential (modified from [6]).

A.3. Synaptic transmisaion

The chemical synapses which are the most widely distributed, transmit informations from a neuron to the other one by means of a neurotransmitter. The neurotransmitters can be divided into three classes: the amino acids, the amines and the peptides. The two firsts are small molecules like for instance glutamate or GABA (gamma-amino butyric acid) for the amino acid or noradrenalin or acetylcholine for the amine. The last class, the peptides, is a chain of amino acids and differs in several ways from the other transmitters. The synapses are constituted of the presynaptic membrane separated by the synaptic cleft (20-50 nm wide) to the postsynaptic membrane. The presynaptic area in the intracellular side of the membrane contains synaptic vesicles, which store the neurotransmitter, and pyramidal structures, called active zone, around which the neurotransmitter is released. Many synapses have also bigger vesicles called secretory granules located a little farther of the synaptic cleft and containing the peptide. These parts are schematised on fig. A.5. When the action potential arrives in a synapse, a voltage gated channel is opened near the active zone: the Ca^{2+} channel. According to the table 1, calcium ions enter into the cell and induce the emission of the neurotransmitter by a process called exocytosis. The membrane of vesicles fuses with the presynaptic membrane and their content spreads out inside the synaptic cleft. The peptides are emitted in the same way but a high frequency train of action potential is required and the exocytosis needs more time. Each neuron releases one amino acid or one amine and eventually one peptide. Receptors are distributed in the postsynaptic membrane and their activation by the neurotransmitter induces several effects. The first kind of receptors is transmitter gated ion channel: when the neurotransmitter, either an amino acid or an amine, activates it, the channel opens allowing ions to pass through. According to the ions which can go

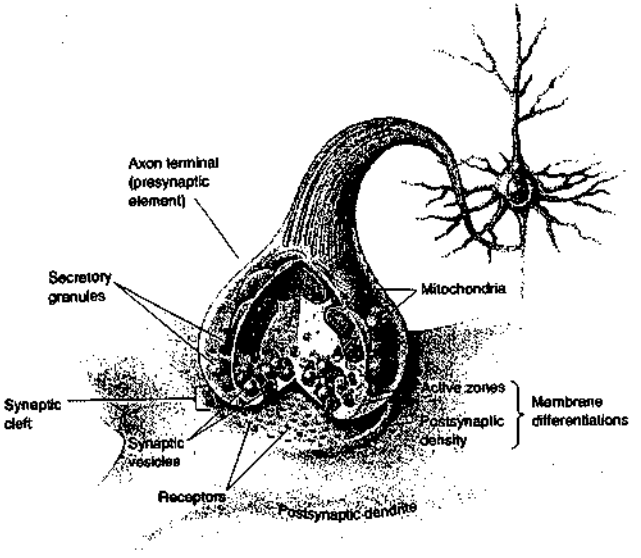

Fig A.5. Scheme of a synapse (from [4]).

through the postsynaptic membrane, two effects are observed. If for instance Na^+ can enter, as for a glutamate gated ion channel, the membrane will cause a depolarisation called excitatory postsynapitc potential (EPSP). If Cl^- can enter, as for the GABA gated ion channel, the membrane will cause an hyperpolarisation called inhibitory postsynapitc potential (IPSP). The second kind of receptor are the G-protein coupled receptors. First the neurotransmitter binds on this receptor, then the G-proteins which move freely in the inner side of the membrane, are activated. These G-proteins can now activate at they turn effector proteins which can be either G-protein gated channel or enzyme which will synthesise molecules called second messenger. Each time that an intermediate is involved, an amplification takes place by activating several elements. These G-protein coupled receptors could induce a lot of metabolic effects as well as change the proprieties of some channels.

There are typically several thousands receptors on a neuron and these receptors are sensible to different neurotransmitters. The action of a neurotransmitter depends on the receptor: for instance a same neurotransmitter can have an excitatory effect on one type of receptors and an inhibitory effect on another one. The coordinated influence of all these inputs induces a resulting action potential if the depolarisation is sufficient. If an action potential has the same shape during all its course, an EPSP is attenuated in reason of the membrane leakage. That is why the position of the synapse, the morphological shape of the postsynaptic neuron and the properties of the membrane have to be taken into account. A synapse can be placed anywhere on the neuron, either on a dendrite or on the soma or also on the axon, changing its efficiency. For instance, a unique EPSP located at the extremity of a long thin dendrite has few chances to induce an action potential. With the coordinated influence of the synapses, voltage summation of two types can take place; spatial summation: if several excitatory input occur together, and temporal summation if a succession of action potentials arrive in the same axon in a short time. In both cases, the resulting depolarisation will be increased. The IPSP's use Cl^- channels for which the equilibrium potential is E_{Cl^-} = -65 mV. If the membrane potential is depolarised at one place, the IPSP will decrease its value toward the resting membrane potential. These kind of synapses can compensate the positive charge in the inner side of the membrane by a negative charge, in a process called shunting inhibition. Moreover these inhibitory synapses are often placed on the soma where their efficiency is enhanced. The G - protein coupled receptors which are not always connected to the opening of channels, can change some of their proprieties by the means of second messengers. As a consequence the efficiency of the other synapses is changed. This effect, referred to as modulation, can also be either excitatory or inhibitory and makes that the previous events change the proprieties of the neuron. Some receptors are also located in the axon terminal of the presynaptic neuron. These

receptors, called autoreceptors, can regulate the release of neurotransmitters if required. The binding of the neurotransmitter on a receptor, like all the other chemical steps involved in synaptic transmission, can be affected by drugs. The molecules which prevent the normal function of a receptor are called receptor antagonists. On the opposite, those imitating the neurotransmitter effect are called receptors agonists. For instance, the receptor type $GABA_A$ can be blocked by the receptor antagonist Picrotoxin, avoiding the inhibition which should take place when GABA is released on this receptor [2]. As a consequence, the neuron enters in epilepsy, as shown in paragraph 4.5.

References

1 J. G. N. Nicholls, A. R. Martin, and B. G. Wallace "From Neuron to Brain", Sinauer associates, Sunderland (USA), 1992

2 G. M. Shephard "The Synaptic Organisation of the Brain" Oxford University press, New York (USA), 1990

3 E. R. Kandel, J. H. Schwrtz, T. M. Jessell, "Principles of neural science", Appleton & Lange, East Norwalk (USA), 1991

4 M. F. Bear, B. W. Connors, and M. A. Paradiso "Neuroscience: exploring the brain", Williams & Wilkins, Baltimore (USA), 1996

5 D. A. Stenger and T. M. McKenna "Enabling technologies for cultured neural networks" academic press, San Diego (USA), 1994

6 J.-M. Robert "Comprendre notre cerveau" éditions du seuil, Paris (France), 1982

7 A. J. Bard and L. R. Faulkner "Electrochemical Methods: Fundamentals and Applications", John Wiley and Sons, New York (USA), 1980

8 J. Koolman and K. -H. Röhm "Color Atlas of Biochemistry", Thieme, Stuttgart (Germany), 1996, p 105

Acknowledgements

This thesis was realised thanks to the help of many people who are here gratefully acknowledged. First of all, I would like to thank Prof. Milena Koudelka-Hep for having given me the opportunity of working in her team. Her scientific and human qualities created an exceptional environment in which I greatly appreciated to be involved. Her pertinent advices and her continuous support throughout this work were of an invaluable help. I also thank Prof. Nico de Rooij for having welcomed me in his efficient and stimulating group.
I would like to thank Dr. Marc-Alexis Grétillat, Dr. Georges-André Racine and Dr. Christian Linder for having taught me the microtechnology and for having introduced me to the fabrication laboratory. I would like to address a special thank to Dr. Cynthia Beuret for her close collaboration on this project thank to the silicon tip technology. I am very grateful to her for all the interesting discussions we had and for her friendship since the early stage of our studies. I also thank Laurent Dellmann and Sylvain Roth for their advices concerning the thick photoresist technology. I would like to express my gratitude to the members of the "Electrochemical Microsystems" group, Dr. Philippe Arquint, Dr. Jean-Charles Fiaccabrino, Dr. Marco Meijerink, Dr. Philippe Michel, Dr. David Strike, and Dr. Peter van der Wal for their assistance on so many subjects. I also thank Dr. Bart van der Schoot for his advices on microfluidic. A special thank to the technical team, Sylvain Jeanneret, Bastien Droz, Sabina Jenny, Gianni Mondin, José Vaquera and particularly Sylviane Pochon for the innumerable encapsulations and Pierre-André Clerc notably for his immeasurable contribution on DRIE. I would like to thank Mathias Schulze, Christophe Kottelat and Claudio Novelli for their computer support and Antoinette Goumaz-Rebetez and Margrit Rüegg for their administrative help.

The SAMLab's members are here sincerely acknowledged for all the help they provided which had no direct connection with this work. They were a friendly team and it has been a great pleasure to work with them. Therefore I warmly thank Dr. Terunobu Akiyama, Dr. Nicolas Blanc, Marc Boillat, Danick Briand, Dr. Jürgen Brugger, Laura Ceriotti, Dr. Antoine Daridon, Bas de Heij, Arash Dodge, Philippe Dubois, Dr. Karl Fluri, Dr. Volker Gass, Sebastien Gautsch, Dr. Florence Grétillat, Olivier Guenat, Benedikt Guldimann, Lutz Haase, Dr. Pierre-François Indermühle, Dr. Victor Jaecklin, Dr. Eva L'Hostis, Gian Luca Lettieri, Jan Lichtenberg, Dr. Philippe Luginbuhl, Dr. Cornel Marxer, PD Wrener Morf, Dr. Wilfried Noell, Dr. Lionel Paratte, Grégor Schürmann, Dr. Urs Staufer, Dr. Sabeth Verpoorte.

I would like to send my best wishes to Luca Berdondini who will go on working on this subject in the future.

I would also like to thank Claude Ketterer (CSEM) and Prof. Diehl (Institute of Biology, University of Neuchâtel) for the SEM photographs

This development has required a lot of collaboration with other research laboratories. I would like to express my gratitude to Dr. Stoppini at the University of Geneva (Switzerland) and to all the people involved in the European project "*In vitro* neurotoxicology tests based on the coupling of brain slices to silicon microelectrode arrays" leaded by Prof. Massimo Grattarola, Department of Biophysical and Electronic Engineering, University of Genoa (Italy) who kindly accepted to be co-examiner of this thesis. The persons involved in this European project are Dr. Sergio Martinoia and Marco Bove, Department of Biophysical and Electronic Engineering, University of Genoa (Italy), Dr. Maurizio Balestrino and Renata Rebaudo, Department of Neurology, University of Genoa (Italy), Prof. Giambattista Bonanno, Institute of Pharmacology and Pharmacognosy, University of Genoa (Italy), Dr. Henrik Jahnsen, Department of Medical Physiology, University of Copenhagen (Denmark), Dr. Rüdiger Köhling, Institute of Physiology, University of Münster

(Germany), Prof. Jens Zimmer, Birthe Jakobsen, Bjarne Kristensen and Jens Noraberg, Department of Anatomy and Cell Biology, University of Odense (Denmark) and Yves Dupont, Bio-Logic Instrument S. A. (France). The Financial support via grant OFES 97.0279 is here gratefully acknowledged.

I would like to address a special thank to Manon Bois who carefully corrected my English in this thesis.

Finally, I would like to thank my parents for their constant support which notably allowed me to study and to complete this thesis.

List of publications

Book contribution

P. Thiébaud, P. Arquint, B. H. van der Schoot, N. F. de Rooij, and M. Koudelka-Hep "Les microsystèmes analytiques (μ-TAS)" in N. Jaffrezic, E. Souteyrand, C. Martelet, S. Cosnier, P. Labbe, and C. Pijolat "Les capteurs chimiques" (ISBN 2-907922-51-3), chap. V, p.212-224

Refereed articles

D. J. Strike, P. Thiébaud, A. C. van der Sluis, M. Koudelka-Hep, and N. F. de Rooij "Glucose measurement using a micromachined open tubular heterogeneous enzyme reactor (MOTHER)" Microsystem technologies, vol. 1, 1994, p. 48-50

M.-A. Grétillat, P. Thiébaud, C. Linder, and N. F. de Rooij "Integrated circuit compatible electrostatic polysilicon microrelays" Journal of micromechanics and microengineering, vol. 5, 1995, p. 156-160

D. J. Strike, P. Thiébaud, P. Arquint, M. Koudelka-Hep, N. F. de Rooij, and M. G. H. Meijerink "Glucose and Urea Measurement using micromachined open tubular heterogeneous enzyme reactors" DECHEMA Monographs, vol. 132- VCH Verlagsgesellschaft, 1996, p. 125-137.

D. J. Strike, M. G. H. Meijerink, P. Thiébaud, P. Arquint, and N. F. de Rooij "Micromachined enzymatic reactors" MST News: international activities in microsystem technology, n°17, 1996, p. 4

M.-A. Grétillat, F. Paoletti, P. Thiébaud, S. Roth, M. Koudelka-Hep, and N. F. de Rooij "A new fabrication method of borosilicate glass capillary tubes with lateral inlets and outlets" Sensors and Actuators, vol. A60, 1997, p. 219-222

L. X. Tiefenauer, S. Kossek, C. Padeste, and P. Thiébaud "Towards amperometric immunosensor devices" Biosensors & Bioelectronics, vol. 12, 1997, p. 213-223

P. Thiébaud, N. F. de Rooij, M. Koudelka-Hep, and L. Stoppini "Microelectrode arrays for electrophysiological monitoring of hippocampal organotypic slice cultures" IEEE transactions on biomedical engineering, vol. 44, 1997, p. 1159-1163

P.-A. Clerc, L. Dellmann, F. Grétillat, M.-A. Grétillat, P. F. Indermühle, S. Jeanneret, P. Luginbuhl, C. Marxer, T. L. Pfeffer, G.-A. Racine, S. Roth, U. Staufer, C. Stebler, P. Thiébaud, and N. F. de Rooij "Advanced deep reactive etching: a versatile tool for microelectromechanical systems" Journal of micromechanics and microengineering, vol. 8, 1998, p 272-278

P. Thiébaud, C. Beuret, M. Koudelka-Hep, M. Bove, S. Martinoia, M. Grattarola, H. Jahnsen, R. Rebaudo, M. Balestrino, J. Zimmer, and Y. Dupont "An array of Pt-tip microelectrodes for extracellular monitoring of activity of brain slices" Biosensors & Bioelectronics, vol. 14, 1999, p. 61-65

H. Jahnsen, B. W. Kristensen, P. Thiébaud, J. Noraberg, B. Jakobsen, M. Bove, S. Martinoia, M. Koudelka-Hep, M. Grattarola, and J. Zimmer "Coupling of organotypic brain slice cultures to silicon-based arrays of electrodes" Methods: a companion to methods in enzymology, vol. 18, 1999, p.160-172 or http://www.idealibrary.com

Conferences snd workshop proceedings

M.-A. Grétillat, P. Thiébaud, N. F. de Rooij, and C. Linder "Electrostatic polysilicon microrelays integrated with MOSFETs" Proceedings IEEE Micro Electro Mechanical Systems (MEMS), 1994, Oiso (Japan), p. 97-101

M.-A. Grétillat, P. Thiébaud, C. Linder, and N. F. de Rooij "IC compatible electrostatic polysilicon microrelays" Workshop digest Micromechanics Europe (MME), 1994, Pisa (Italy), p. 137-140

L. X. Tiefenauer, C. Padeste, S. Kossek, H. W. Lehmann, C. Musil, P. Thiébaud, M. Koudelka-Hep, and J. Gobrecht "Molecular architecture for integrated immunosensor devices" Proceedings European congress on biotechnology, Nice (France), 1995

P. Thiébaud, B. H. van der Schoot, N. F. de Rooij, and M. Koudelka-Hep "Fluidic microsystem for immunosensor integration" Workshop of European Interregional Network on Sensors (EINS), 1995, Neuchâtel (Switzerland)

D. J. Strike, M. G. H. Meijerink, P. Thiébaud, P. Arquint, M. Koudelka-Hep, and N. F. de Rooij "Detection of glucose and urea using miniature enzyme reactors, coupled with a miniature silicon-based electrochemical detector" Workshop of European Interregional Network on Sensors (EINS), 1995, Neuchâtel (Switzerland)

P. Thiébaud, P. Arquint, B. H. van der Schoot, N. F. de Rooij, and M. Koudelka-Hep "Les microsystèmes analytiques (μ-TAS)" École thématique CNRS, march 96, Lamoura (France)

L. X. Tiefenauer, S. Kossek, C. Padeste, and P. Thiébaud "Amperometric immunosensor devices" Award finalist lecture at the 4th World Congress on Biosensors, 1996, Bangkok (Thailand), p. 30

M.-A. Grétillat, F. Paoletti, P. Thiébaud, S. Roth, M. Koudelka-Hep, and N. F. de Rooij "A new fabrication method of borosilicate glass capillary tubes with lateral inlets and outlets" Proceedings of Eurosensors X, 1996, Leuven (Belgium), p. 259-263

M.-A. Grétillat, F. Paoletti, P. Thiébaud, S. Roth, M. Koudelka-Hep, and N. F. de Rooij "A new fabrication method of borosilicate glass capillary tubes with lateral inlets and outlets" Proceedings of the 2nd international symposium on miniaturized total analysis systems (μTAS), 1996, Basel (Switzerland), p. 214

G. C. Fiaccabrino, P. Zwahlen, P. Thiébaud, G.-A. Racine, N. F. de Rooij, and M. Koudelka-Hep "On-chip detection of electrogenerated chemiluminescence of Ru (bpy) at Pt interdigitated microelectrode arrays" Proceedings of the 9th international conference on solid-state sensors and actuators (Transducers), Chicago (USA), 1997, p. 171-174

P. Thiébaud, L. Stoppini, N. F. de Rooij, and M. Koudelka-Hep "Development of microelectrode arrays for electrophysiological monitoring of organotypic slice cultures" Proceedings of the 3rd international conference on cellular engineering, 1997, San Remo (Italy)

P. Thiebaud, N. F. de Rooij, M. Koudelka-Hep, F. Robert, P. Correges, S. Duport, and L. Stoppini, "Simultaneous multi-electrode recording of field potential and extracellular medium monitoring in brain slice cultures" European journal of cell biology, vol. 74, 1997, abstract n° 162, p. 59

P. Thiébaud, C. Beuret, N. F. de Rooij, and M. Koudelka-Hep "Fabricating microelectrode arrays using thin-film and micromachining technologies" international meeting on substrate-integrated microelectrode arrays, Reutlingen (Germany), 1998, p. 40

Biography

Pierre Thiébaud was born on July 8,1970, in Neuchâtel, Switzerland. In 1988, he started his study in physical electronics at the University of Neuchâtel. He received his MSc degree in physical electronics with mention in August 1993. In October of that year he joined the Institute of Microtechnology (IMT) of the University of Neuchâtel as a research and teaching assistant. Up to September 1996, his principal research interest was the microsystems for micro total analysis systems (μTAS). Then, he started his PhD work on microelectrode arrays (MEA) for electrophysiological applications.